Colloquium @ Department of Physics, NTU

Application of diffusion MRI to cancer, heart and brain connectome imaging

March 11, 2014

Wen-Yih Isaac Tseng MD, PhD

Advanced Biomedical MRI Lab
Center for Optoelectronic Medicine
National Taiwan University College of Medicine

Diffusion phenomenon

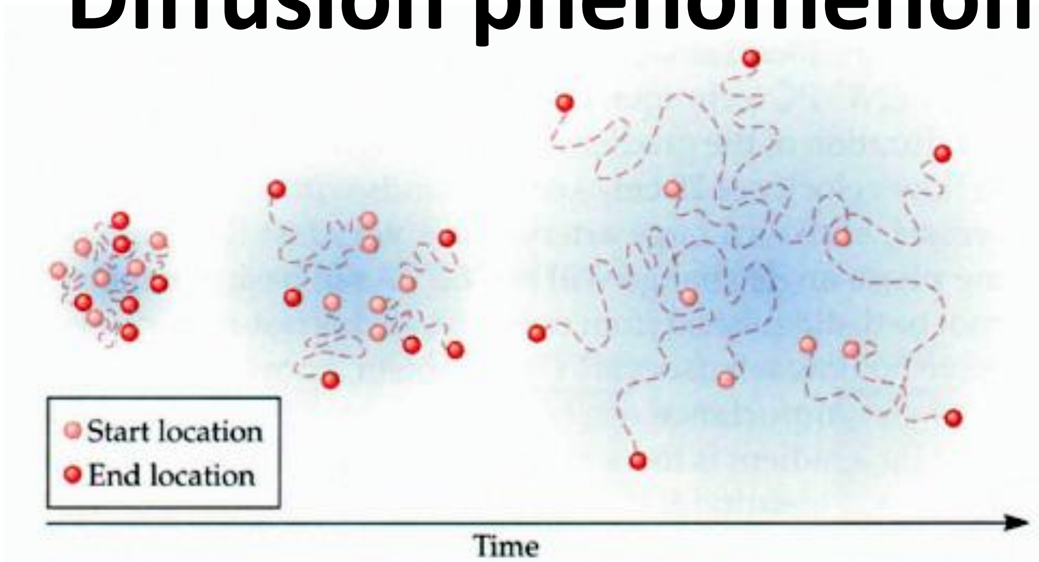

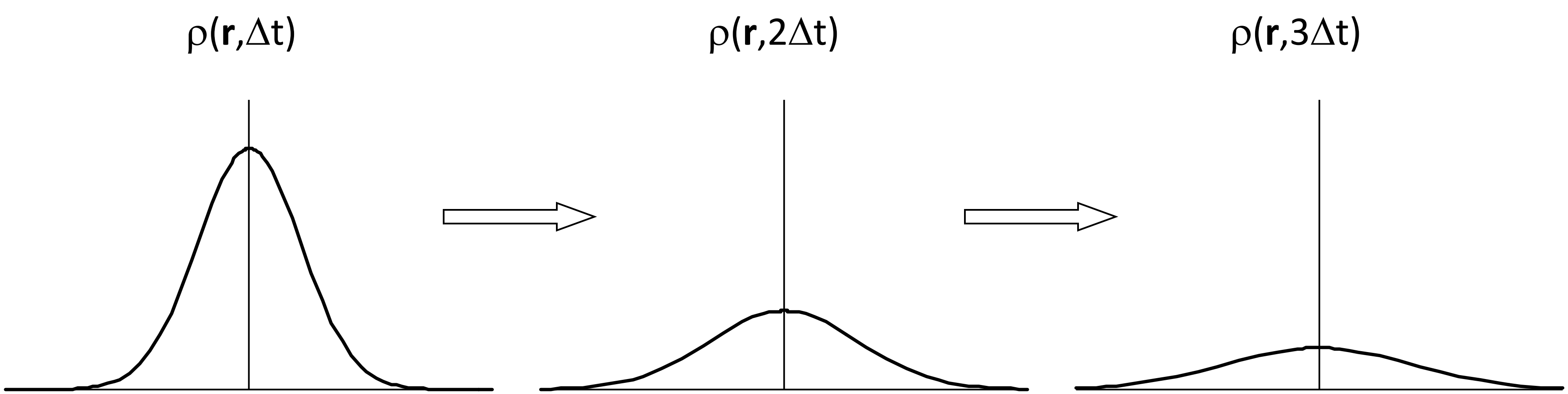

$$\rho(\mathbf{r}',\Delta) = \rho(\mathbf{r},0) * P(\mathbf{r}|\mathbf{r}', \Delta)$$

where $P(\mathbf{r}|\mathbf{r}', \Delta)$ = probability density function

Encoding diffusion with MR

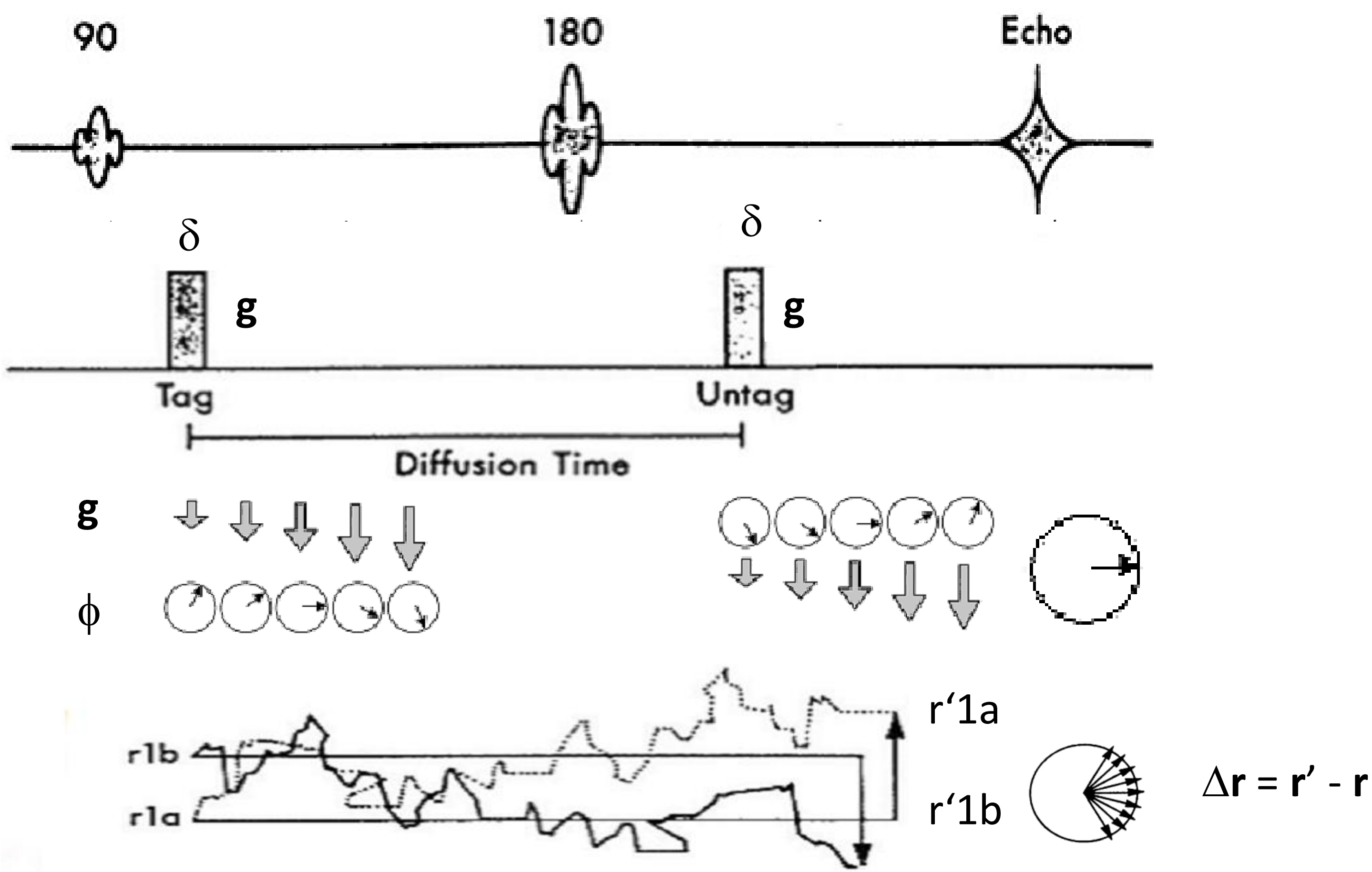

The spin of each proton is endowed by a phase term Exp(i$\Delta\phi$)
where $\Delta\phi = 2\pi\mathbf{q}\cdot(\mathbf{r'} - \mathbf{r})$ and $\mathbf{q} = \gamma\mathbf{g}\delta/2\pi$

Diffusion signal and PDF

Paul T. Callaghan
Principle of nuclear magnetic resonance microscopy 1991

Given $\rho(\mathbf{r}',\Delta) = \rho(\mathbf{r},0) * P(\mathrm{r}|\mathrm{r}', \Delta)$
where the phase term for each spin $\exp(i\Delta\phi) = \exp(i2\pi\mathbf{q}\cdot(\mathbf{r}' - \mathbf{r}))$

$$S(g) = \int_{\mathbf{r}}\int_{\mathbf{r}'} \rho(\mathbf{r}) P(\mathbf{r}|\mathbf{r}', \Delta) \exp\left(i\gamma\delta\mathbf{g}\cdot(\mathbf{r}'-\mathbf{r})\right) d\mathbf{r}'\, d\mathbf{r}$$

$$S(\mathbf{q}) = \int_{\mathbf{r}}\int_{\mathbf{r}'} \rho(\mathbf{r}) P(\mathbf{r}|\mathbf{r}', \Delta) \exp\left(i2\pi\mathbf{q}\cdot(\mathbf{r}'-\mathbf{r})\right) d\mathbf{r}'\, d\mathbf{r}$$

$$S(\mathbf{q}) = \int_{\mathbf{r}} \rho(\mathbf{r})\, d\mathbf{r} \int_{\mathbf{R}} P(\mathbf{R}, \Delta) \exp(i\Delta\phi)\, d\mathbf{R} = S_0 \exp\left(-\left\langle \Delta\phi^2 \right\rangle\right)$$

Diffusion-weighted EPI sequence

Diffusion-weighted

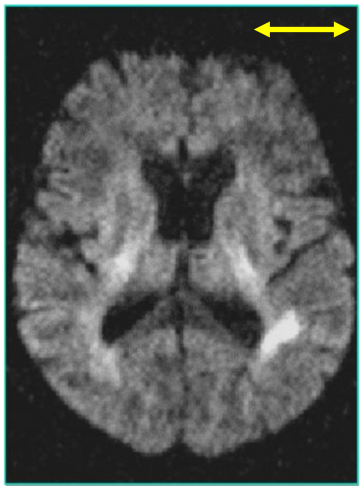

S

T2

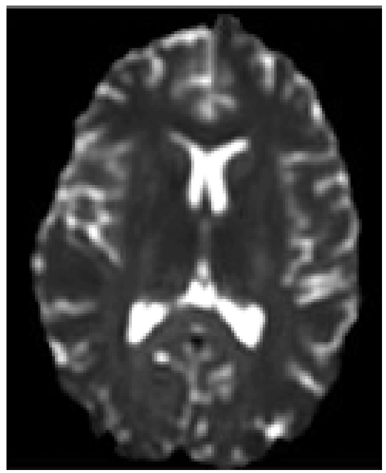

S_0

Sequence

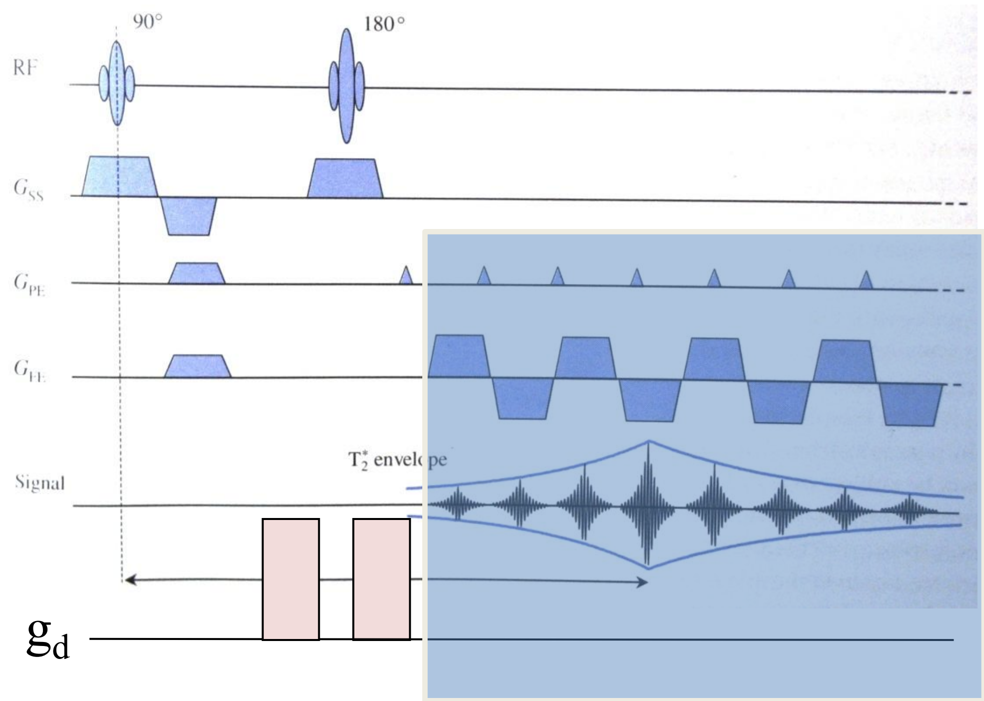

Diffusion Module (q)

Imaging Module (k)

$$S = S_0 \exp^{\left(-(\gamma g \delta)^2 (\Delta - \frac{\delta}{3}) \mathrm{D}\right)} = S_0 \exp^{(-\mathrm{bD})}$$

Diffusion contrast varies with gradient directions

G_{zz}

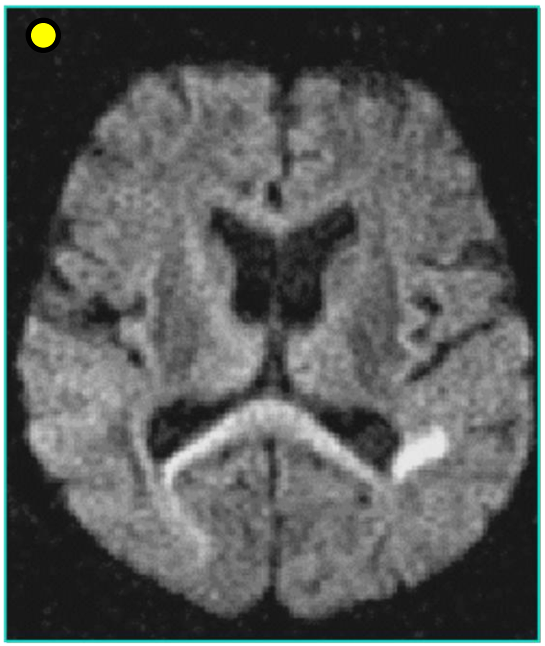

G_{xx}

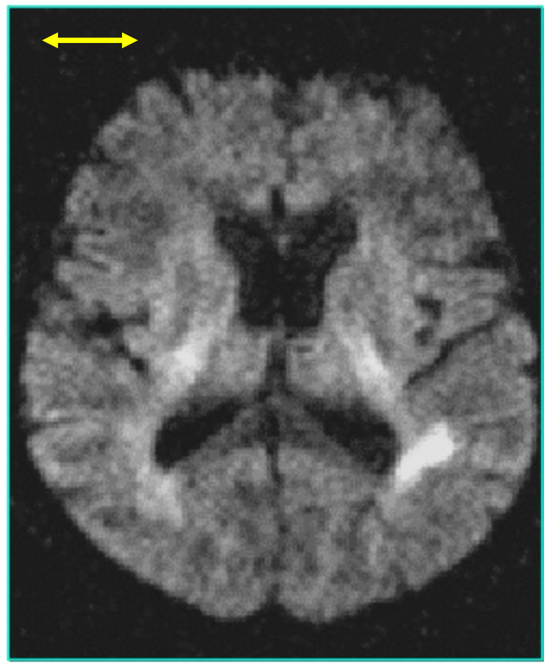

G_{yy}

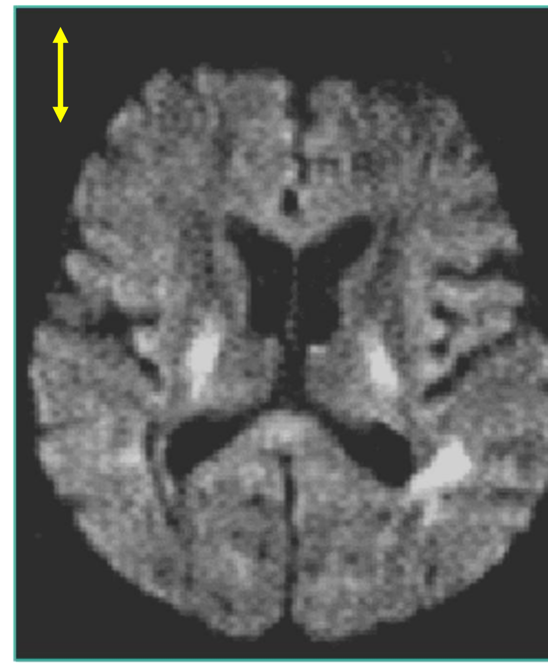

Diffusion-weighted imaging

- In 1990, Moseley et al demonstrated in an animal stroke model that the ADC decreased by approximately 30%-50% within 30 minutes after onset of focal ischemia.
- Sodium ion pumps fail - water goes in cells and can not diffuse – DW image gets bright (note – much later cells burst and stroke area gets very dark).

Conventional T2WI

DW-EPI

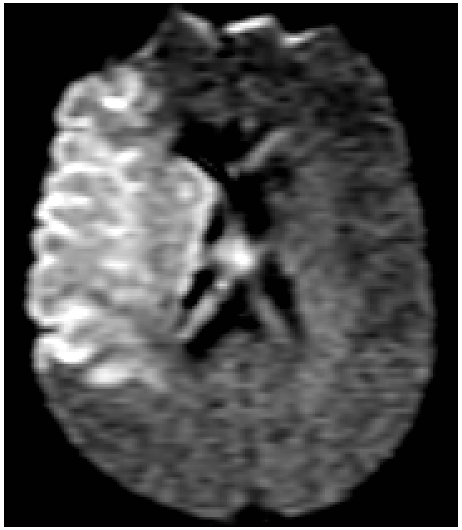

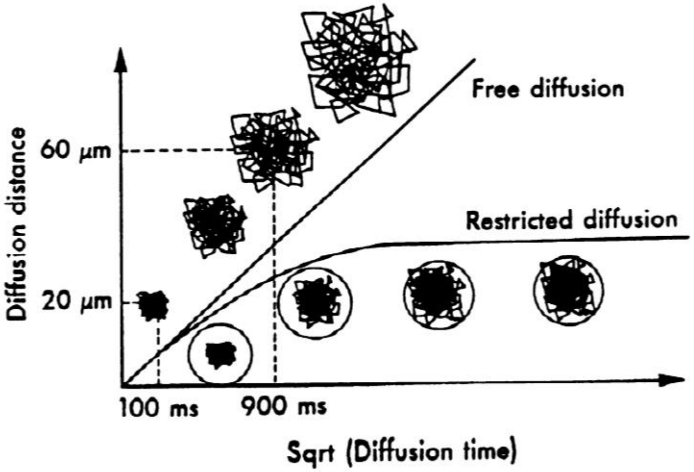

Diffusion anisotropy

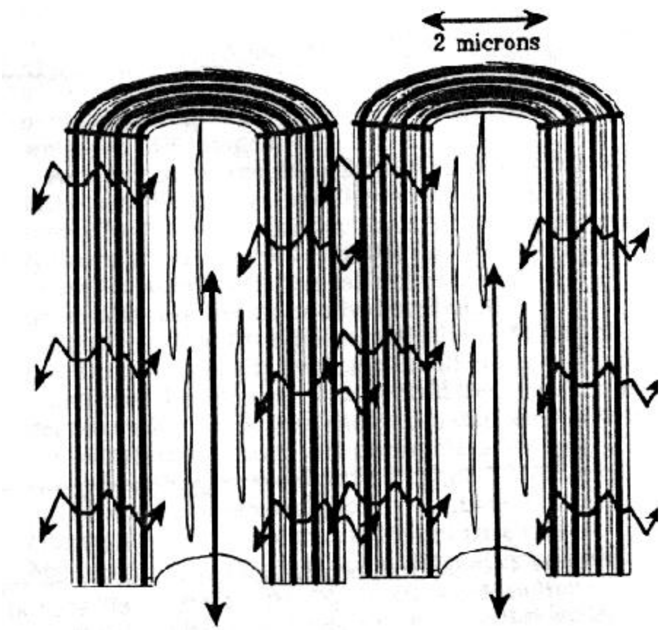

$D_{\parallel} = 1.2 \times 10^{-3}\ mm^2/s$
$D_{\perp} = 0.4 \times 10^{-3}\ mm^2/s$

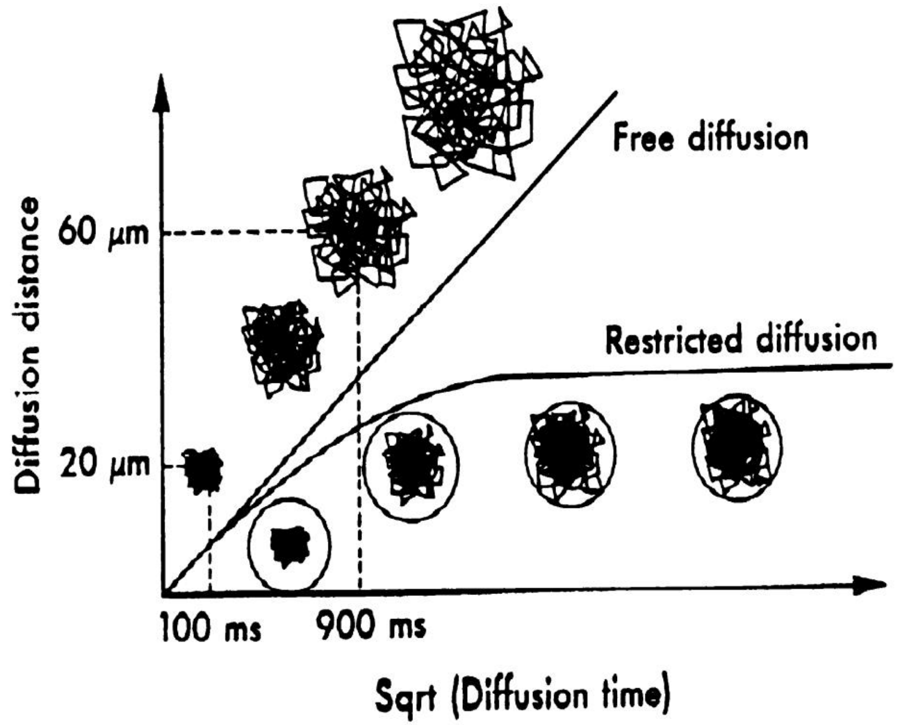

- Douek et al., JCAT 1991

Tensor model for diffusion

isotropic | anisotropic

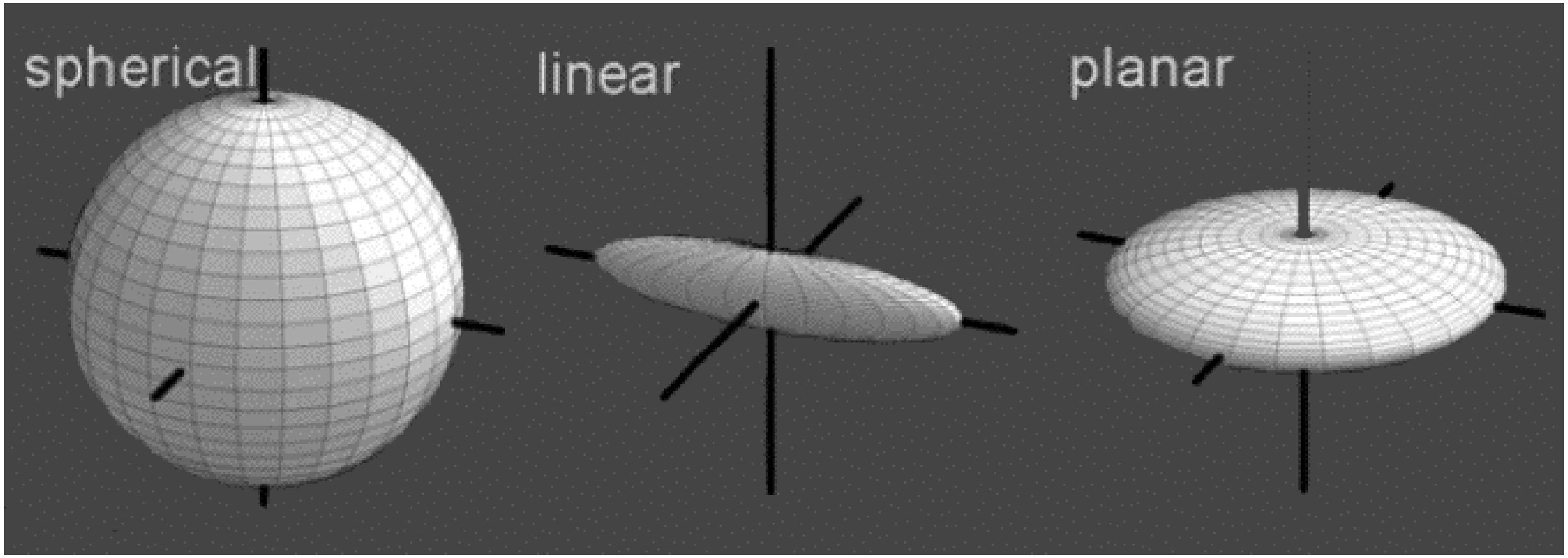

Courtesy: G. Kindlmann

$\lambda_1 = \lambda_2 = \lambda_3$ | $\lambda_1 > \lambda_2 \approx \lambda_3$ | $\lambda_1 \approx \lambda_2 > \lambda_3$

Eigenvectors define alignment of axes

Diffusion tensor imaging (DTI)

Garrido et al. (Circ Res 1994) and Basser et al. (Biophys J 1994)

Diffusion-sensitive gradients

[1 1 0] [1 -1 0] [0 1 1] [0 -1 1]

[1 0 1] [-1 0 1]

$$\ln\left(\frac{S(\mathbf{q})}{S_0}\right) = -\int_0^{TE} \mathbf{q}(t')^T \tilde{D}\mathbf{q}(t')dt' = -\mathbf{b}\tilde{D}$$

$$\tilde{D} = \begin{bmatrix} Dxx & Dxy & Dxz \\ Dyx & Dyy & Dyz \\ Dzx & Dzy & Dzz \end{bmatrix}$$

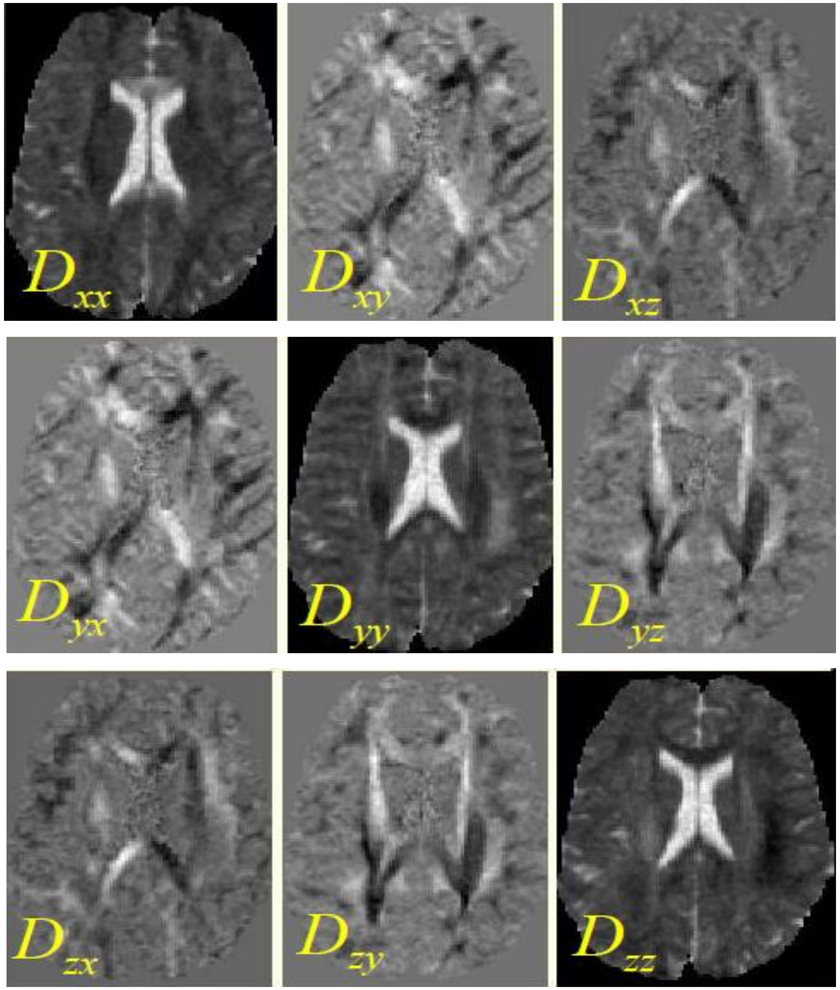

Tensor invariants

- Apparent diffusion coefficient (ADC) $ADC = \frac{\lambda_1 + \lambda_2 + \lambda_3}{3}$

- Fractional anisotropy (FA)

$$FA = \sqrt{\frac{3}{2}} \times \sqrt{\frac{(\lambda_1 - trace)^2 + (\lambda_2 - trace)^2 + (\lambda_3 - trace)^2}{{\lambda_1}^2 + {\lambda_2}^2 + {\lambda_3}^2}}$$

- Principal direction of diffusion tensor *1[st] eigenvector (ev1)*

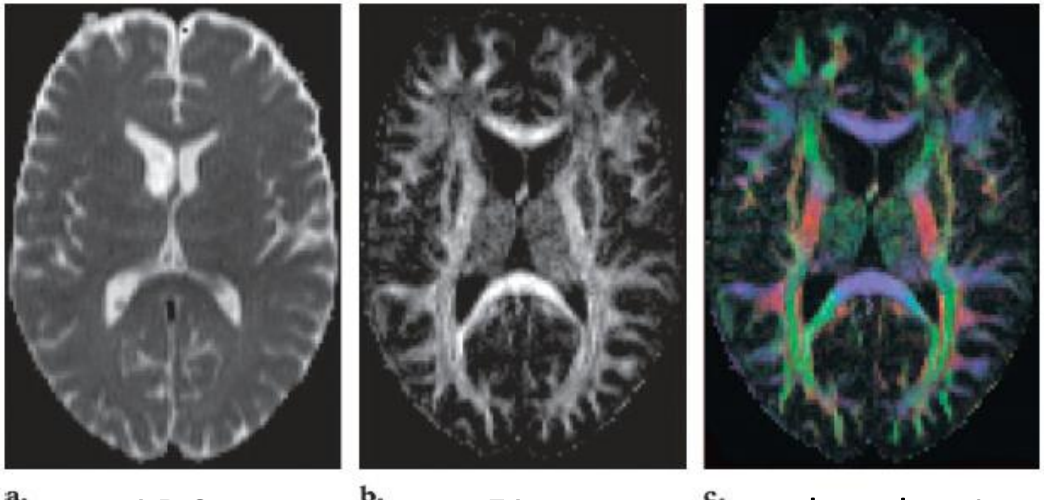

ADC FA colored ev1

First engenvector map

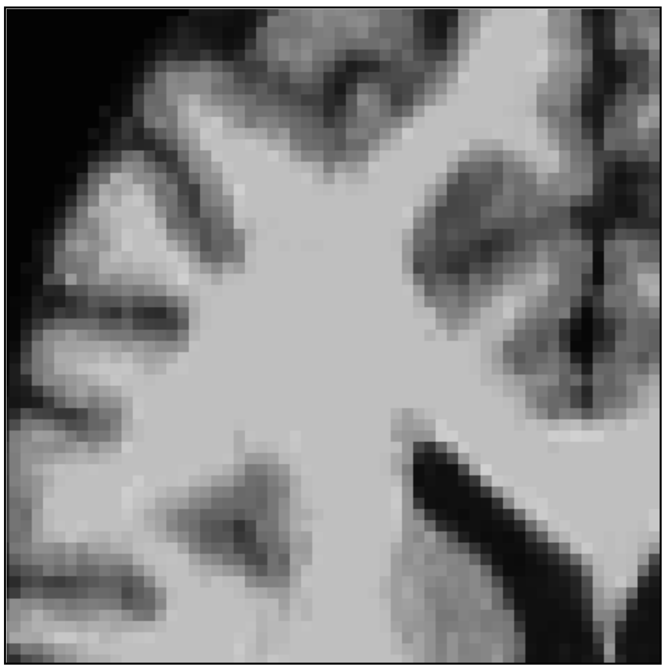

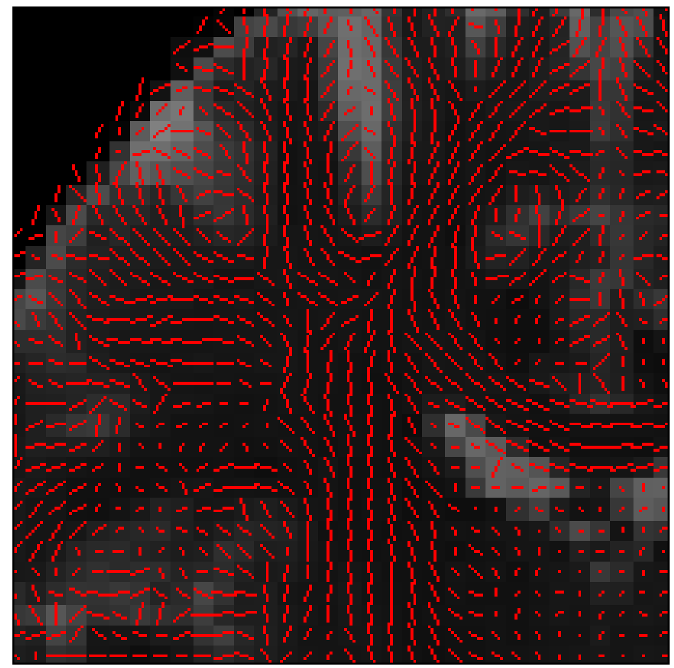

Detection of prostate cancer by ADC

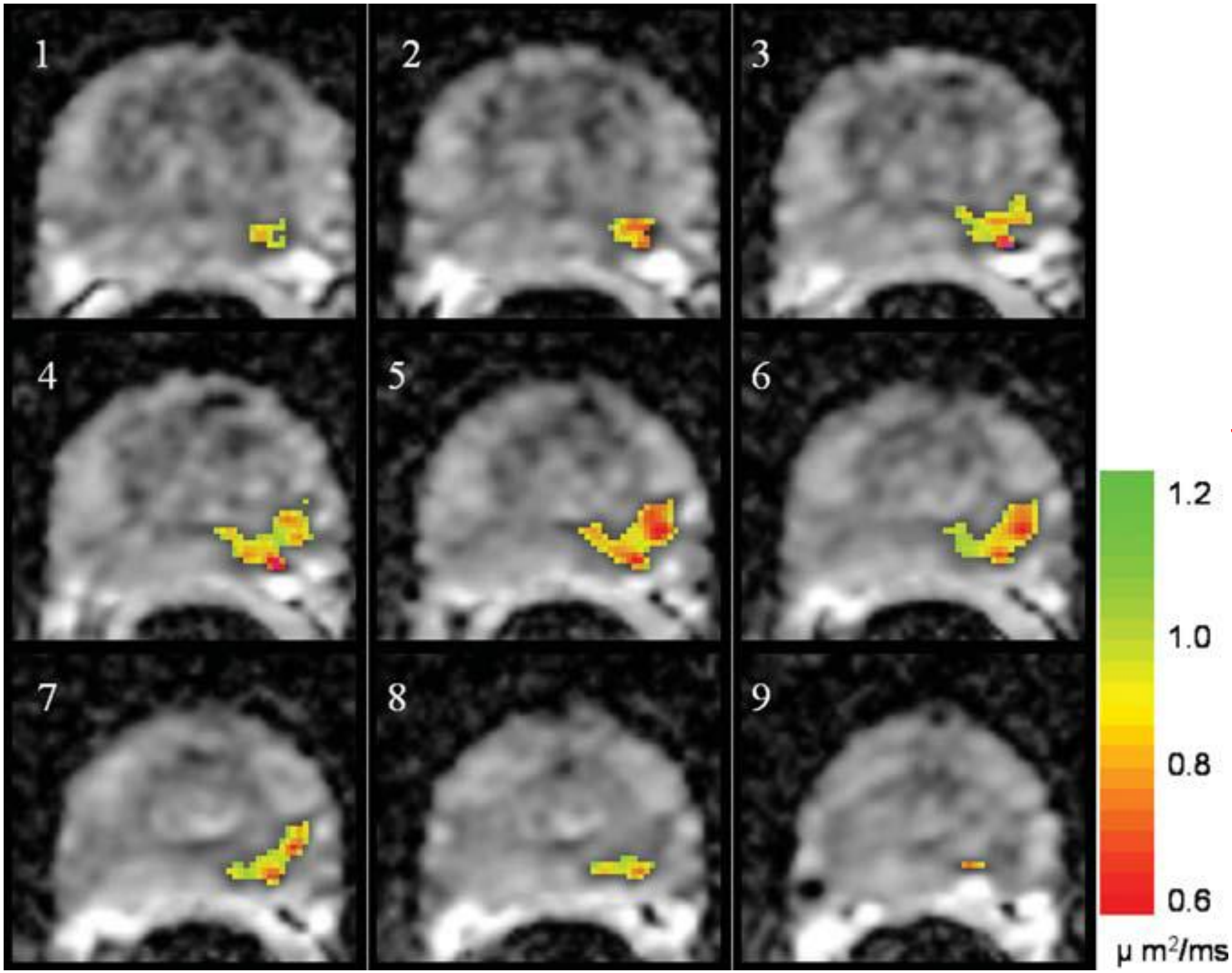

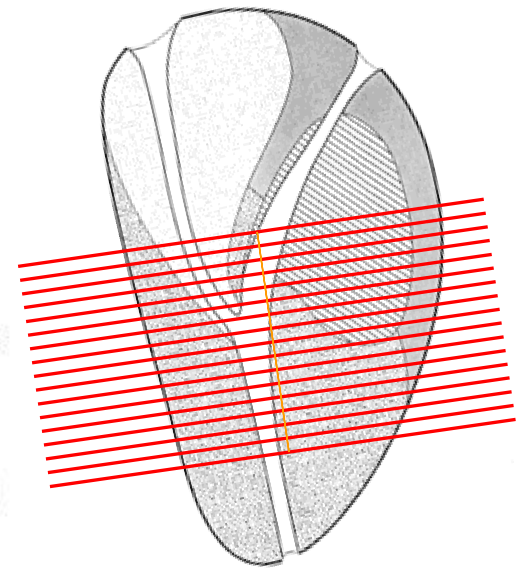

Chen et al. JMRI 2010

ADC correlates with Gleason scores

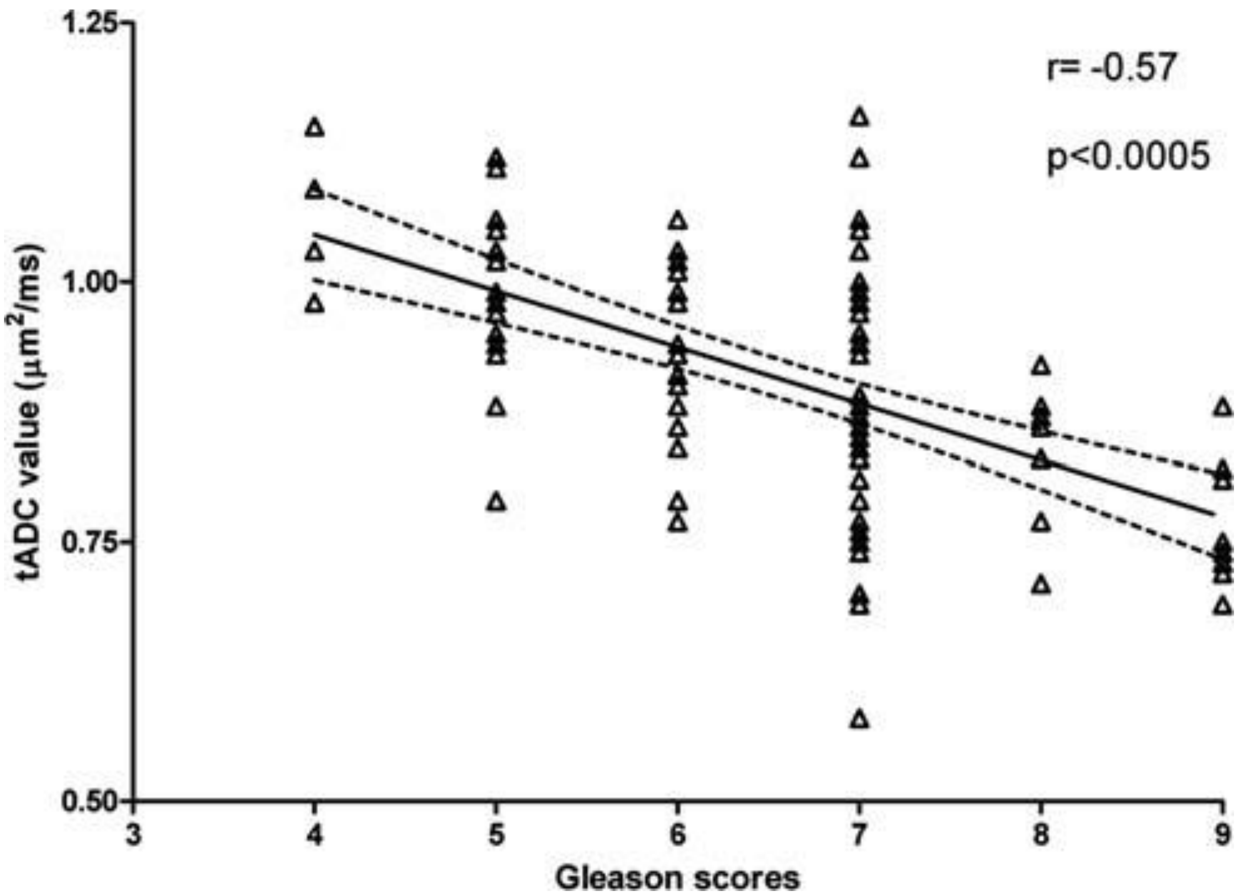

Chen et al. JMRI 2010

Diffusion tensor MRI of normal myocardial fiber architecture

Fiber helix angles (color-code) increase smoothly from epi- to endocardium

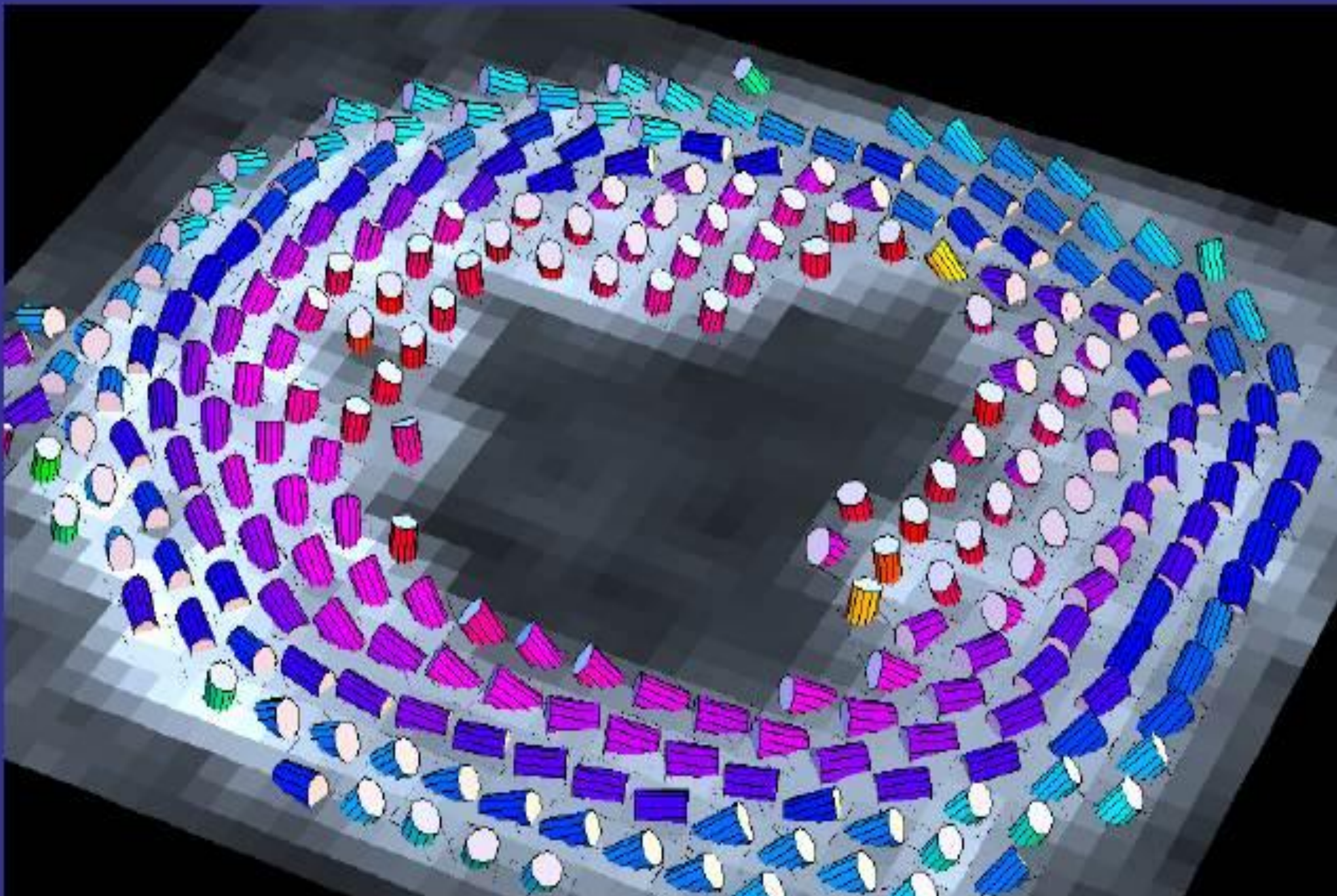

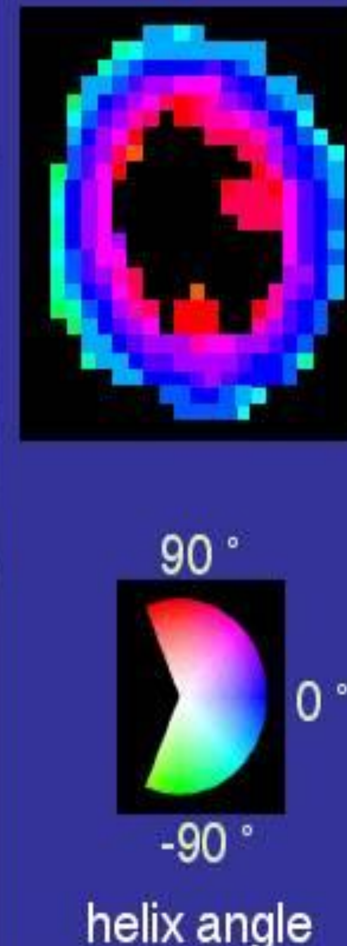

Tseng et al. Radiology 216:128-39;2000

Myocardial fiber archiecture

whole ventricle fibers

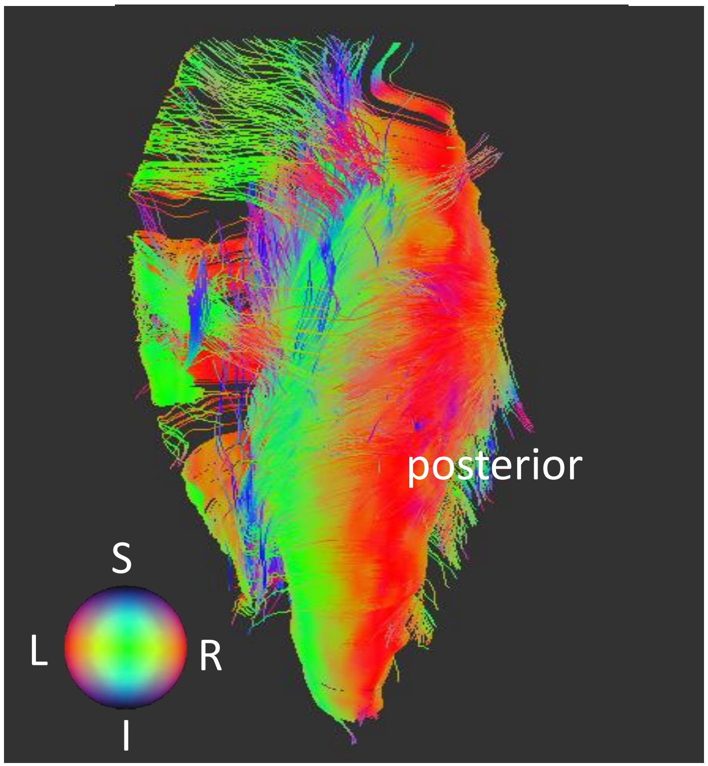

Inner heart **outer heart**

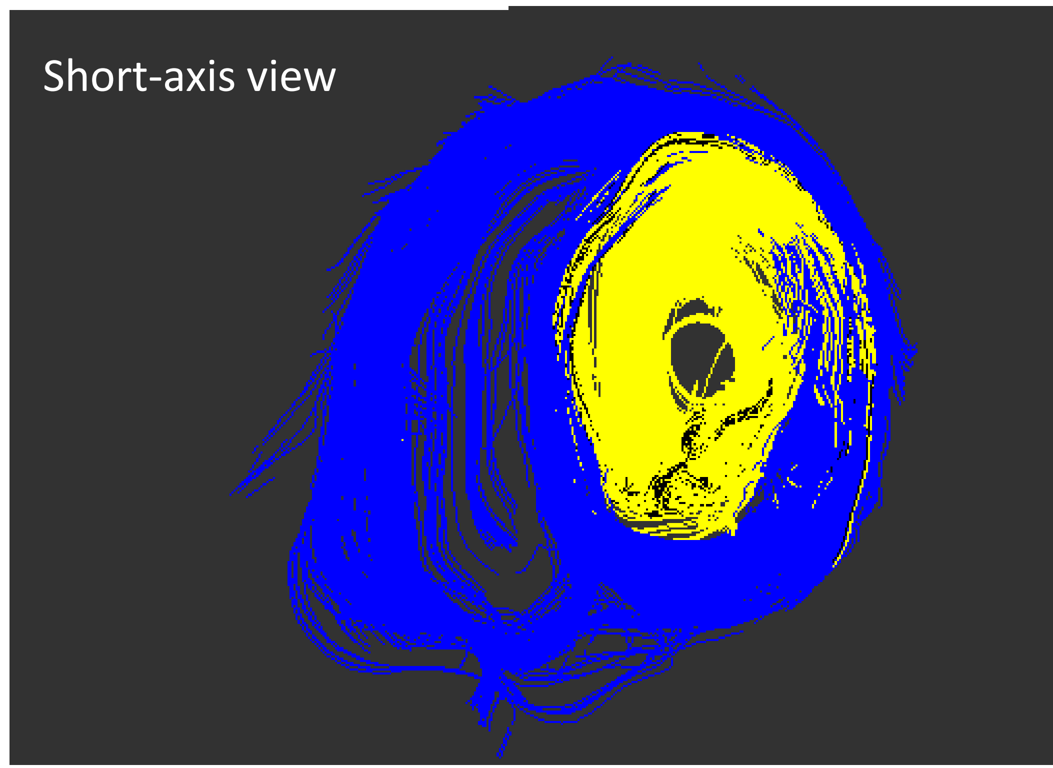

Motion of inner heart system

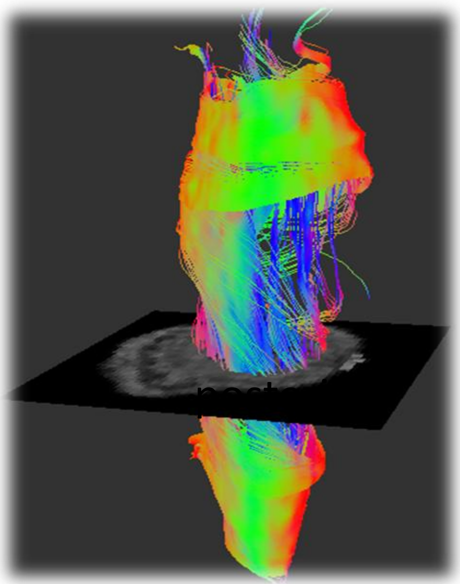

partial fibers of inner heart

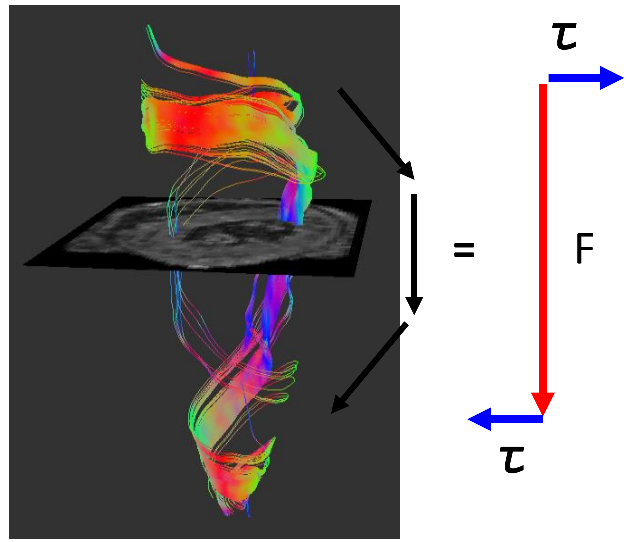

view from base

- Spiral fibers at Apex and Base might contribute to LV **torsion** τ
- Longitudinal fibers in the LV inner wall might contribute to **longitudinal shortening** F

Motion of outer heart system

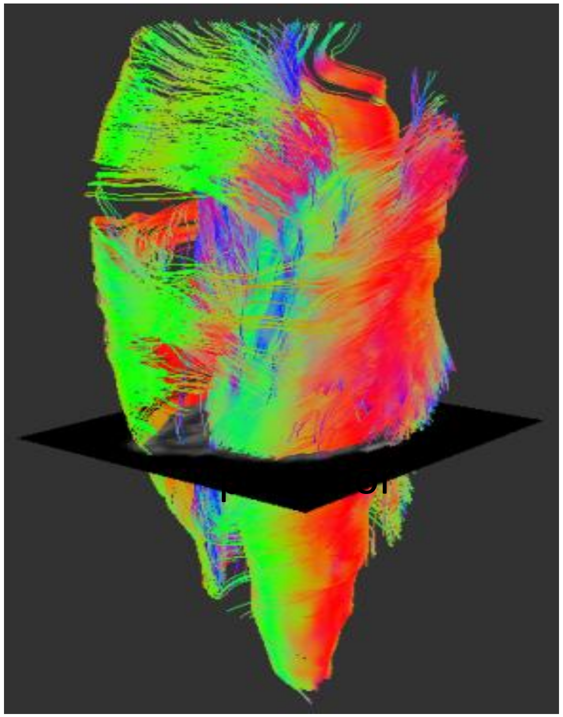

view from base

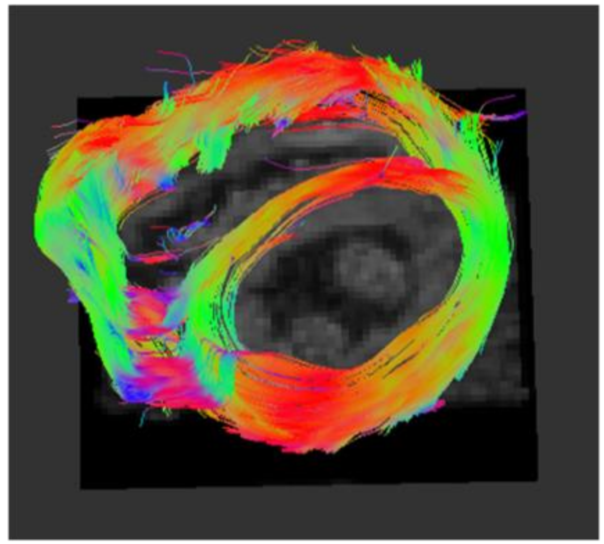

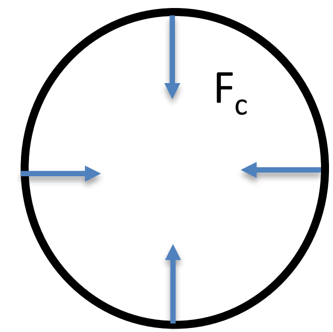

Force of contraction F_c

- Circumferential fibers connecting LV and RV might contribute to **radial contraction** of LV wall F_c

Wendell JS Krieg, 1963

strum is still present. Of the temporal areas, the superior temporal gyrus, 22, in itself a complex area, has a more conventional capsular connection, the stalk fibers passing far back *(D-J)* to enter the retrolenticular capsule. The more caudal are markedly capsular and the more rostral ones have strong orbitofrontal connections **(C, *E*)** The inferior temporal gyrus, 20, has but few connections of any kind, while the middle gyrus, 21, is intermediate in character, but does cross-connect through the anterior commissure. The lenticular nucleus has dwindled but the thalamus has expanded, and the somesthetic nuclei are now in evidence. Ventralis posterior lateralis (VPL), the somesthetic nucleus, receives medial lemniscus fibers from the body and relays to the somesthetic receptive cortex, 3 and 1. The ventralis posterior medialis (VPM), or arcuate nucleus, fits into

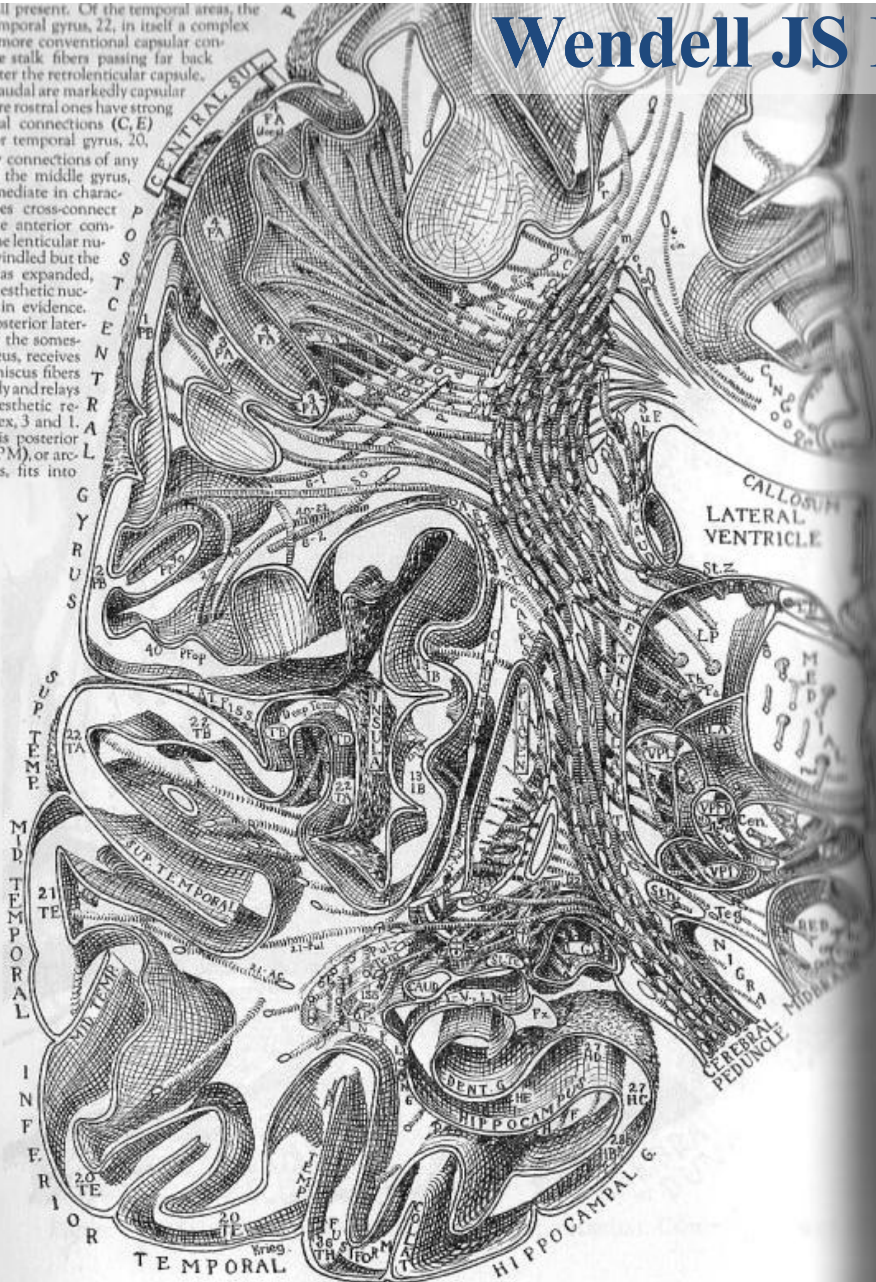

Figure 247. Slice Reconstruction of Human Cerebrum. §G.

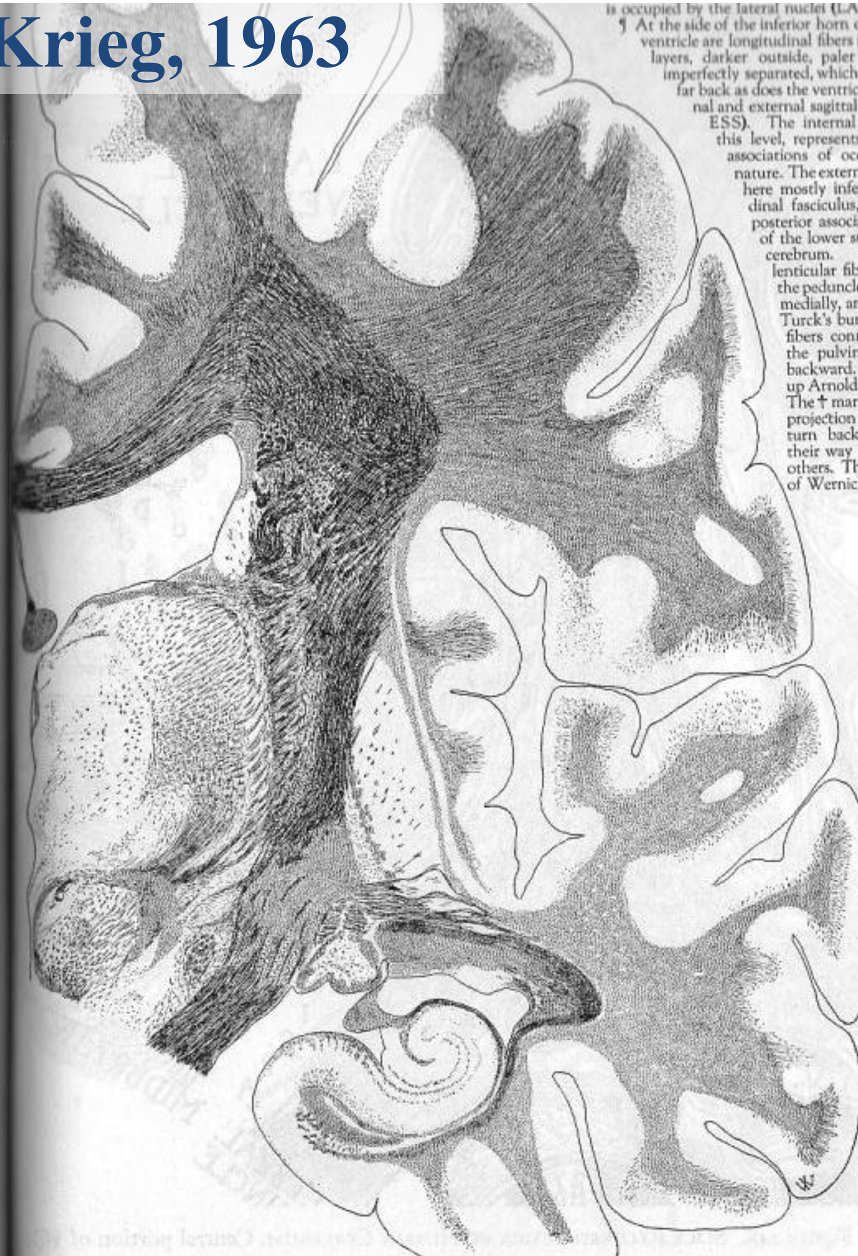

is occupied by the lateral nuclei (LA, LP, LD)
¶ At the side of the inferior horn of the late
ventricle are longitudinal fibers in two th
layers, darker outside, paler inside, l
imperfectly separated, which continu
far back as does the ventricle: the int
nal and external sagittal strata (I
ESS). The internal stratum,
this level, represents principa
associations of occipitofron
nature. The external stratu
here mostly inferior long
dinal fasciculus, the ant
posterior associational la
of the lower surface of
cerebrum. ¶ The in
lenticular fibers that
the peduncle run stra
medially, and consti
Turck's bundle (+).
fibers connecting v
the pulvinar conti
backward. They m
up Arnold's bundle
The † marks the o
projection fibers as t
turn back and we
their way through
others. This is the
of Wernicke.

Diffusion MRI

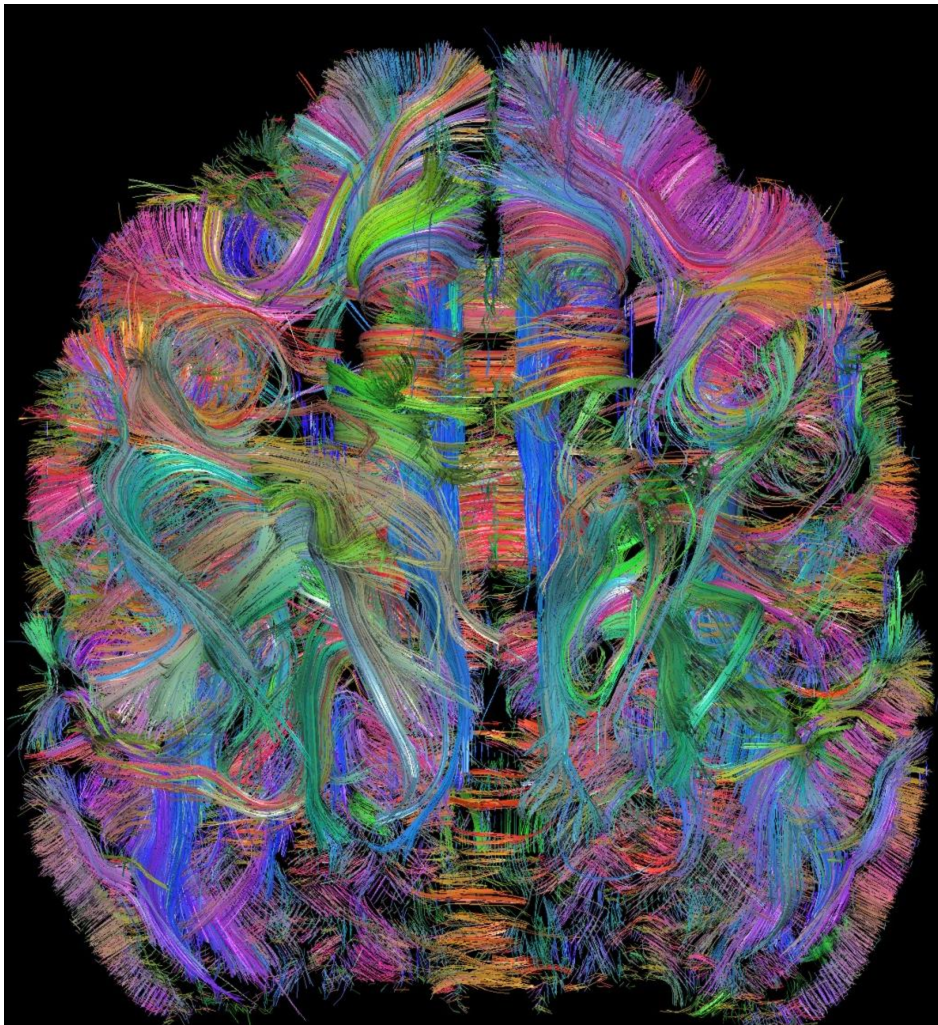

Conventional MRI

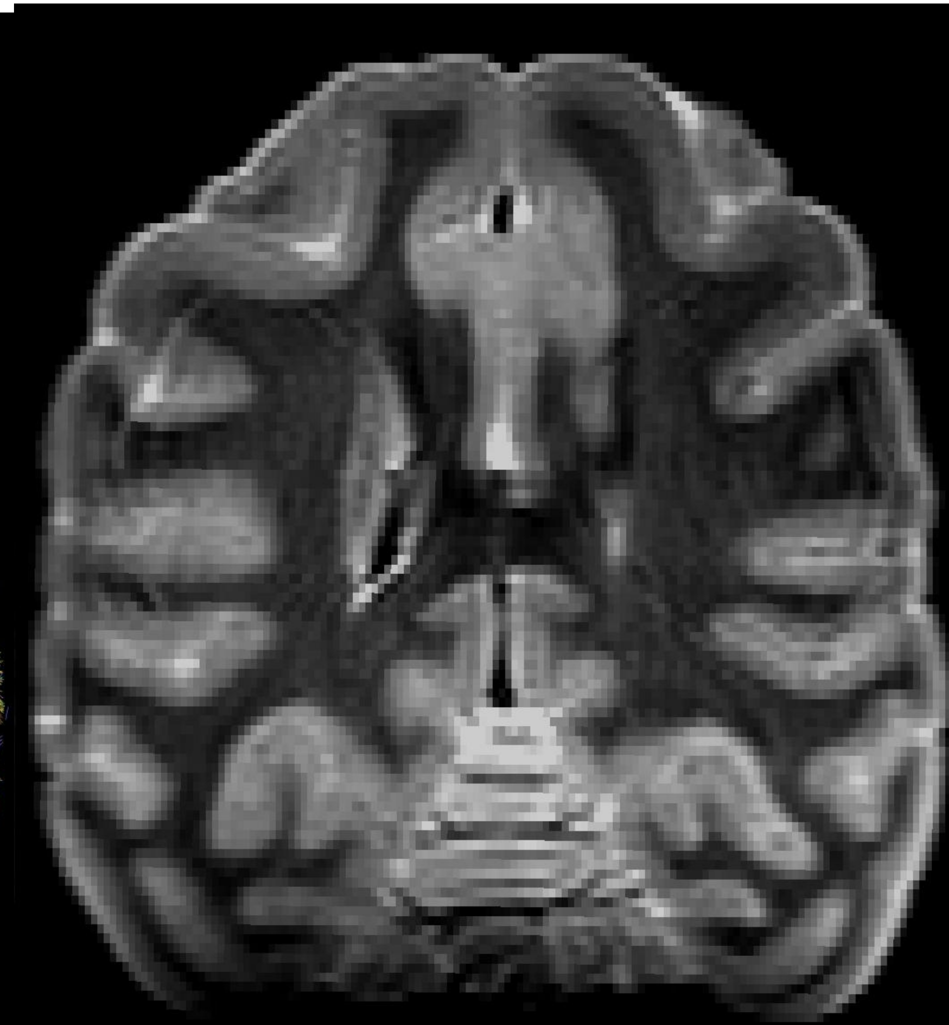

Wedeen, MGH-NMR

Diffusion spectrum imaging

6D (q and k) Space Imaging

$$S(\mathbf{k},\mathbf{q}) = \int \rho(\mathbf{r})\exp(i\ 2\pi\,\mathbf{k}\cdot\mathbf{r})\int P(\mathbf{r},\mathbf{R})\exp(i\ 2\pi\,\mathbf{q}\cdot\mathbf{R})\,d\mathbf{R}\,d\mathbf{r}$$

tissue I(x) | $E(q)$ | $P(r) = FT(E)$ | $ODF(u) = \int r^2 P dr$ | tensor

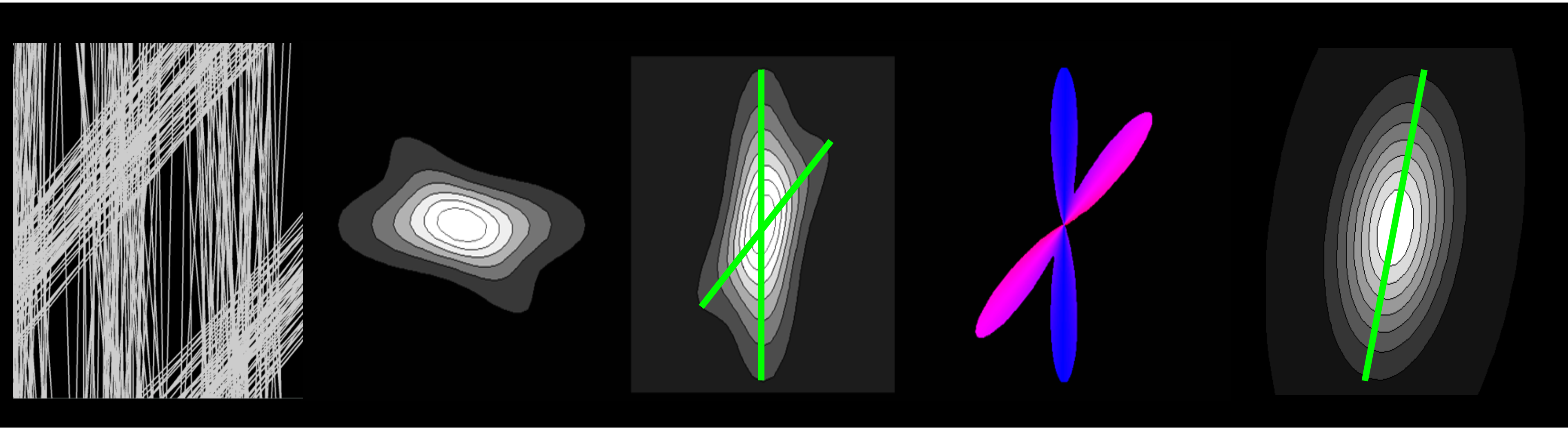

Probability density function | Orientation distribution function

Wedeen, MGH-NMR

DSI acquisition scheme

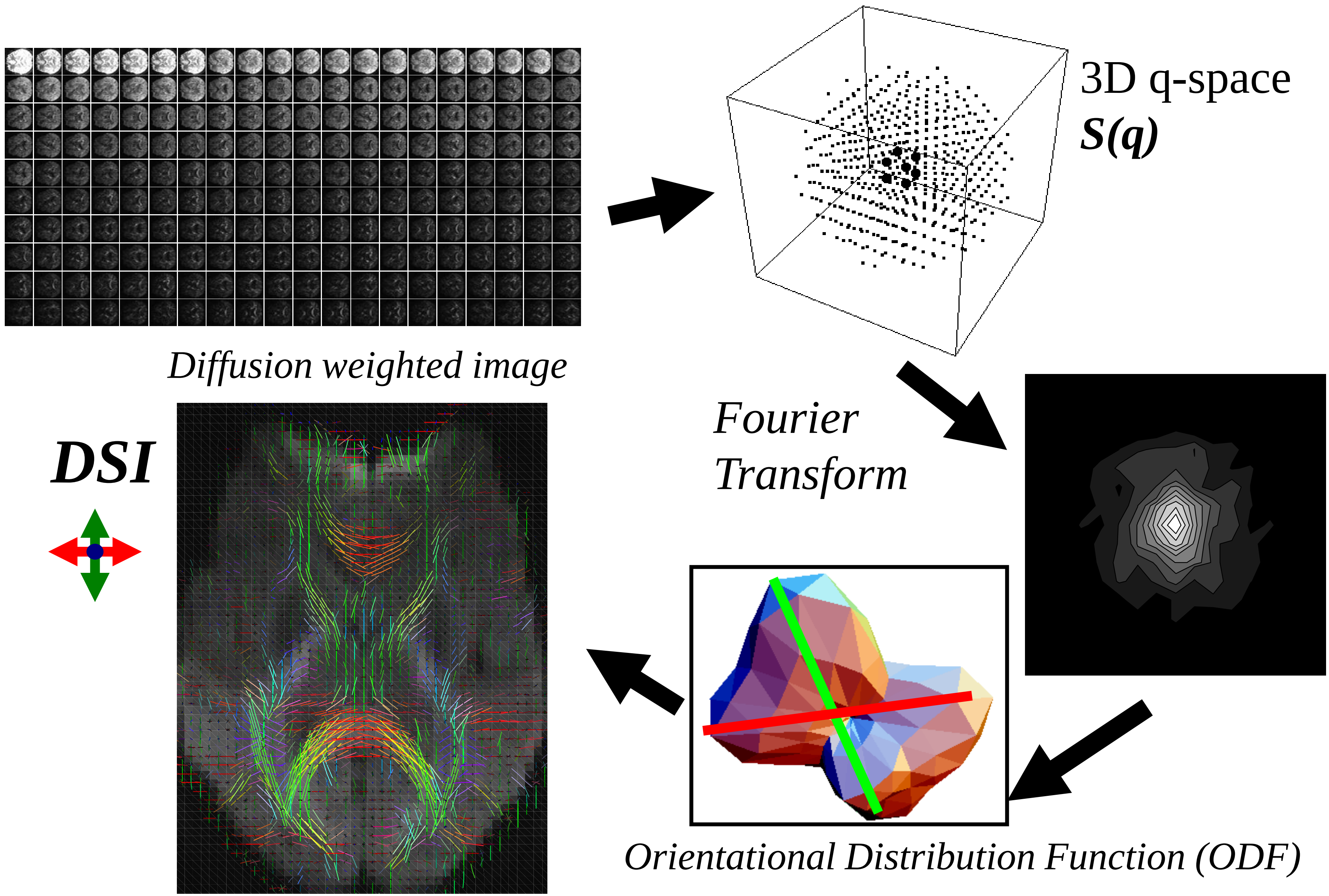

How can we assess white matter integrity from local diffusion information?

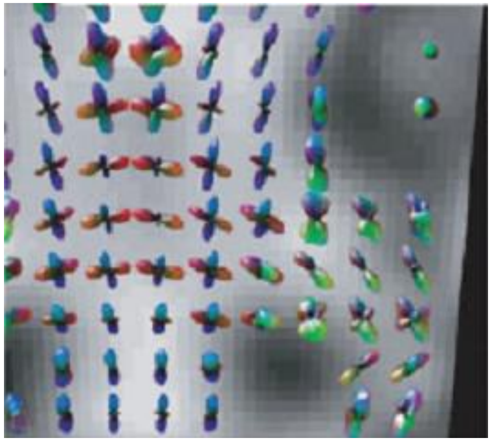

ODF

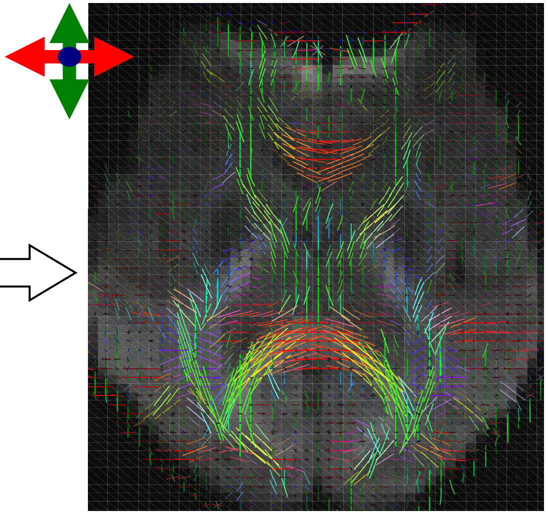

Orientation map

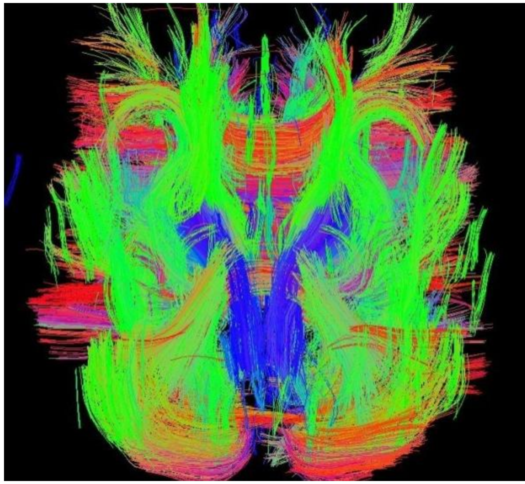

Tractography

Tractography was used to generate connection paths between points in the brain based on local diffusion direction

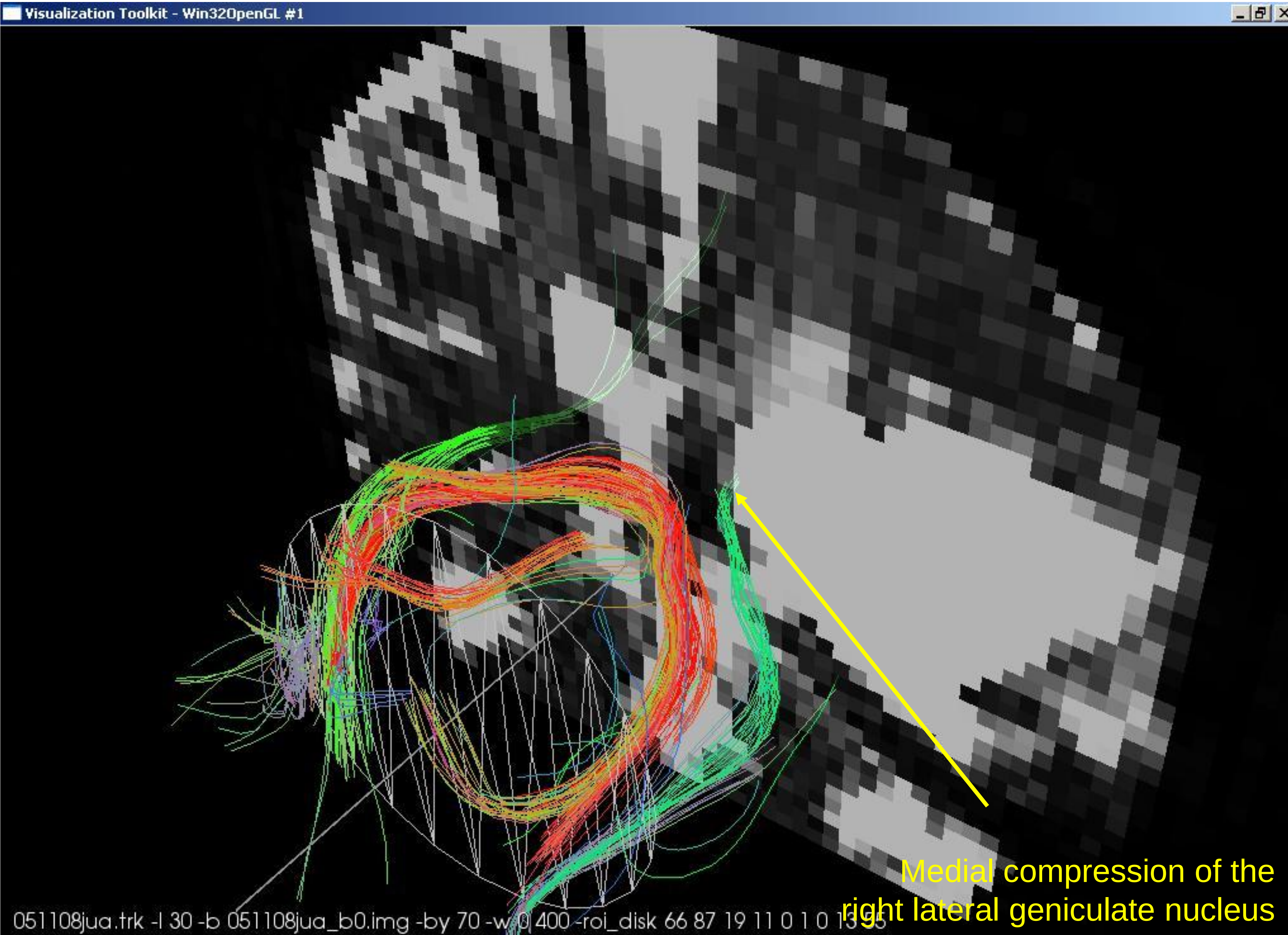
Visualization Toolkit - Win32OpenGL #1
051108jua.trk -l 30 -b 051108jua_b0.img -by 70 -w 0 400 -roi_disk 66 87 19 11 0 1 0
Medial compression of the
right lateral geniculate nucleus

The Geometric Structure of the Brain Fiber Pathways

Wedeen et al. Science 2012;335:1628-34

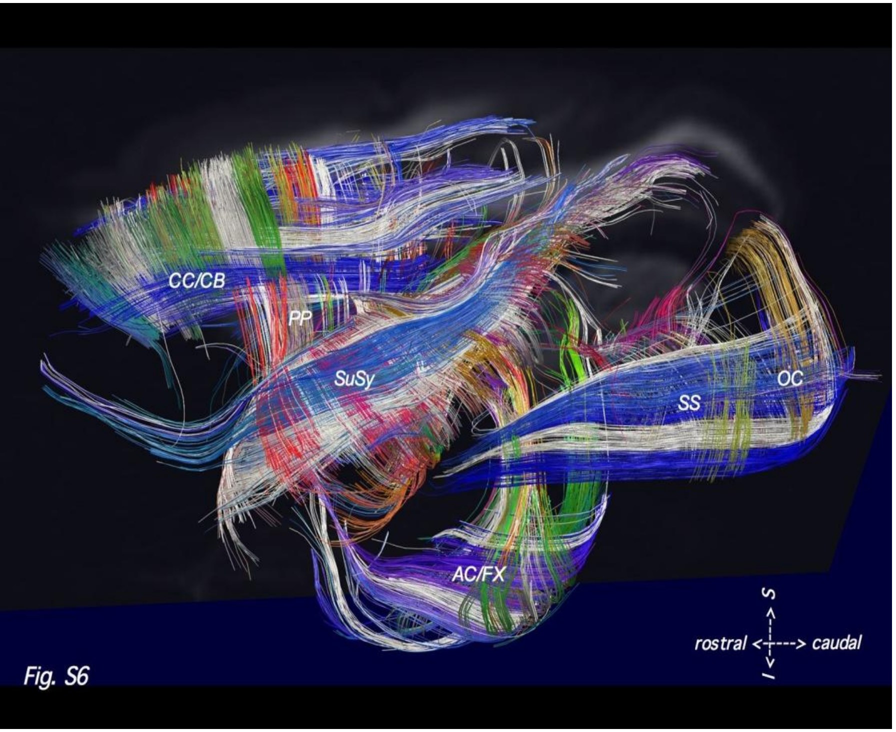

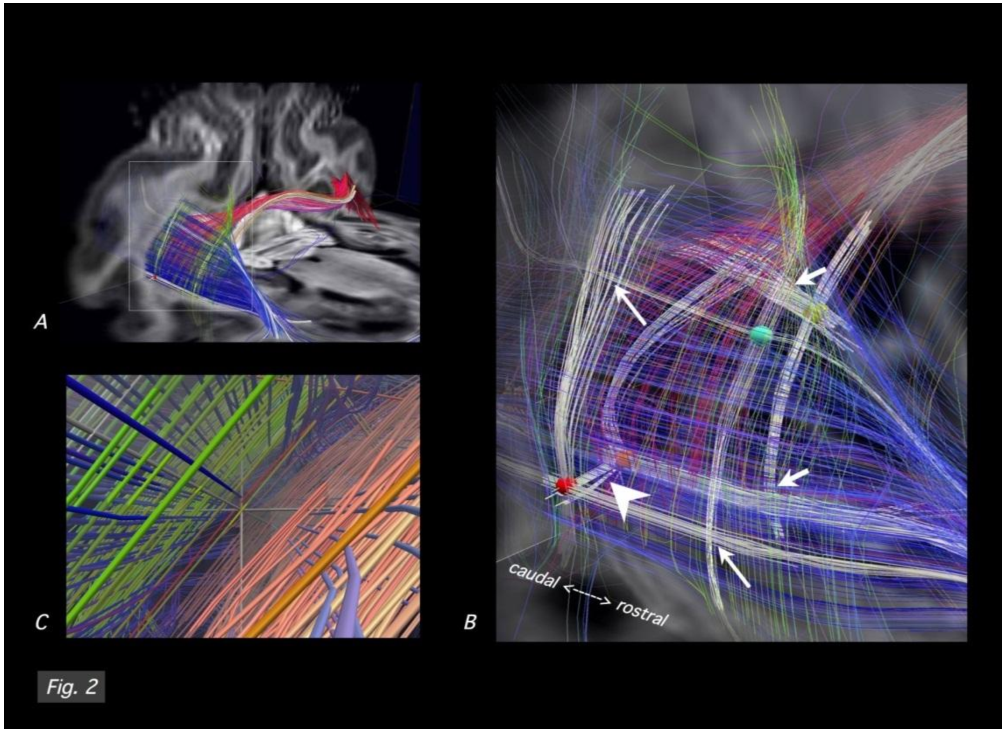

The 3D grid structure in an owl monkey brain

Close-up view of the grid structure in the caudal brain

Fiber grid pattern: also found in human brain

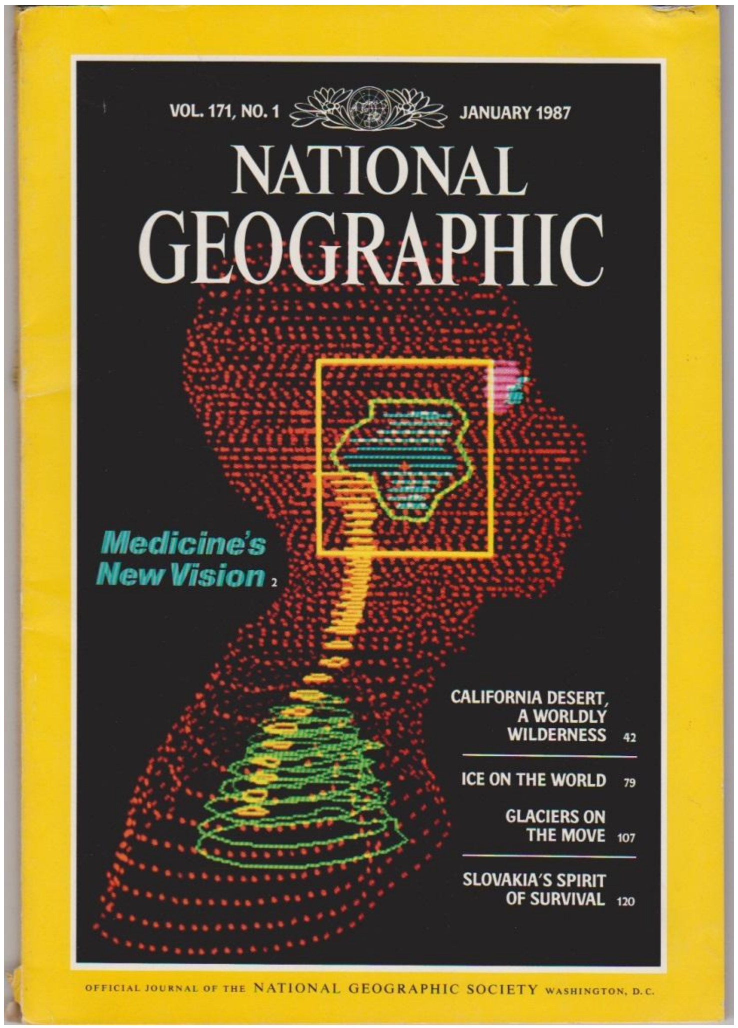

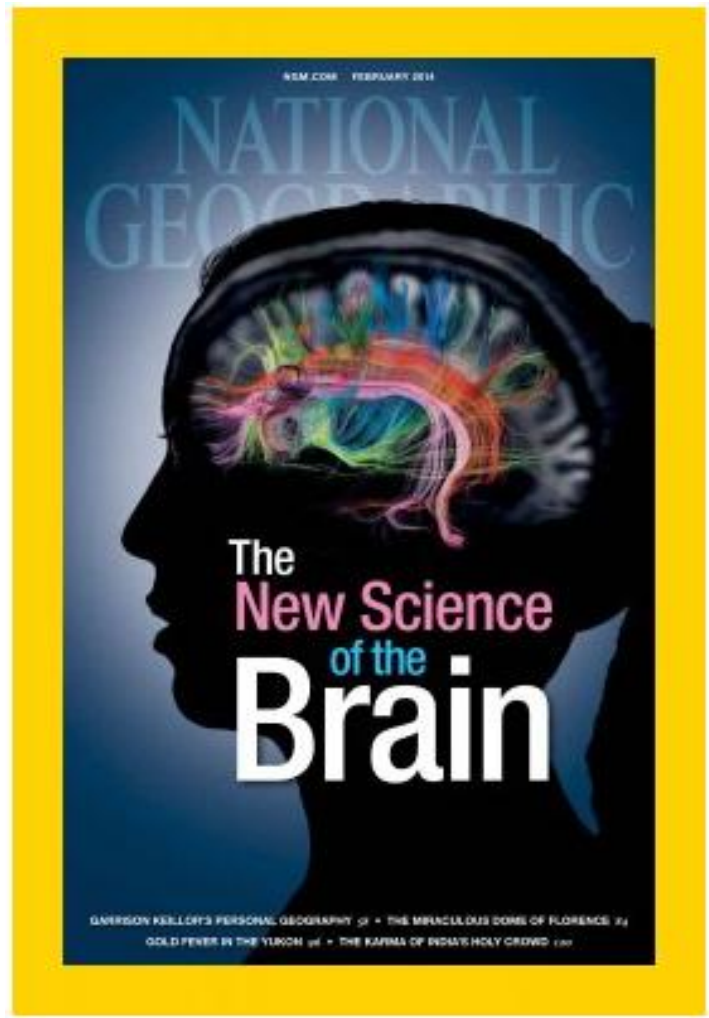

Quantify fiber integrity

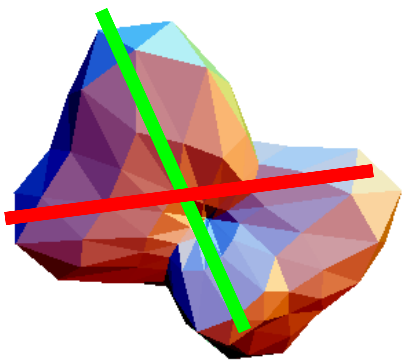

ODF

GFA = SD (ODF)/RMS (ODF)

Generalized fractional anisotropy
Calculated from the ODF

- Degree of myelination
- Directional coherence
- Axonal diameter and density

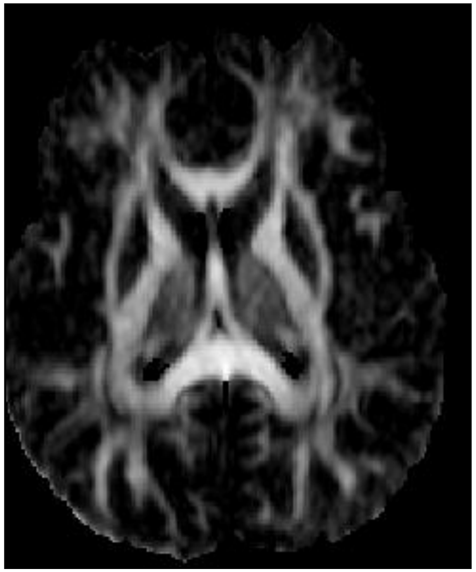

GFA mapping

Mean Path Algorithm

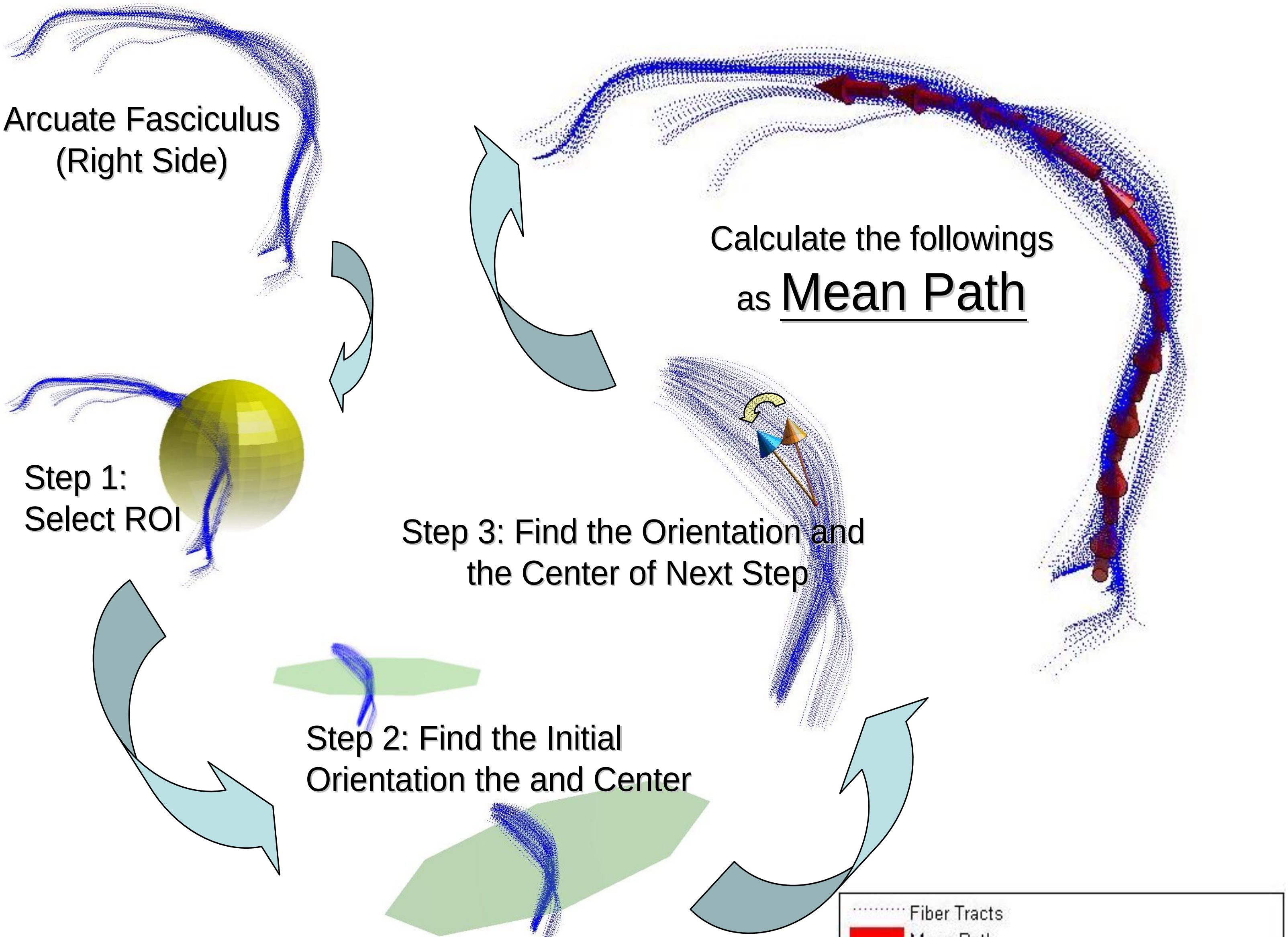

Chiang WY et al. ISMAR 2007

Tract-specific analysis

A

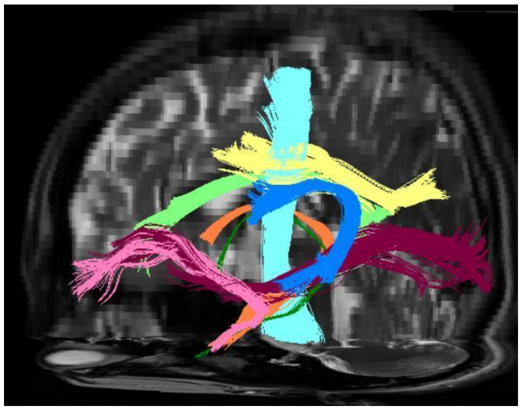

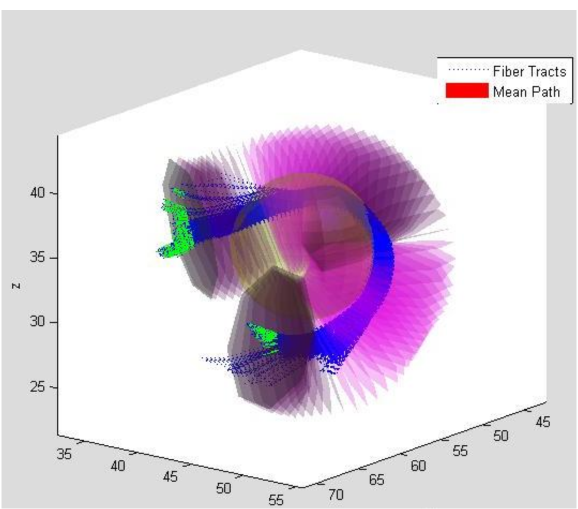

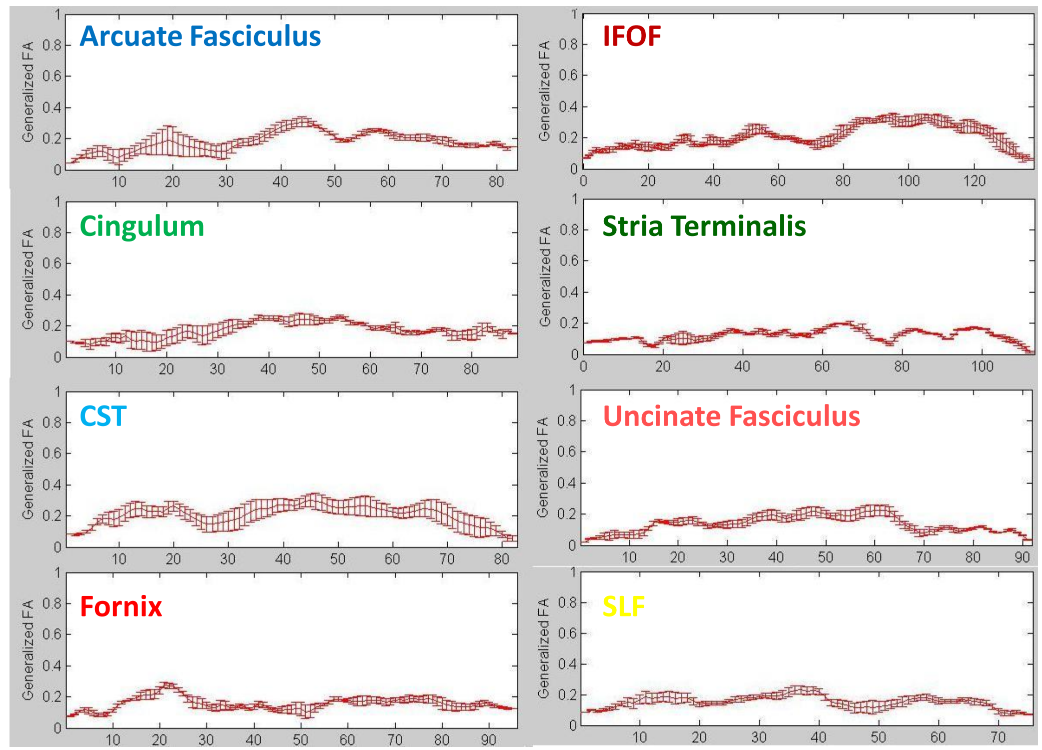

GFA profiles for each fiber tract

Loss of left-greater-than-right asymmetry in autism

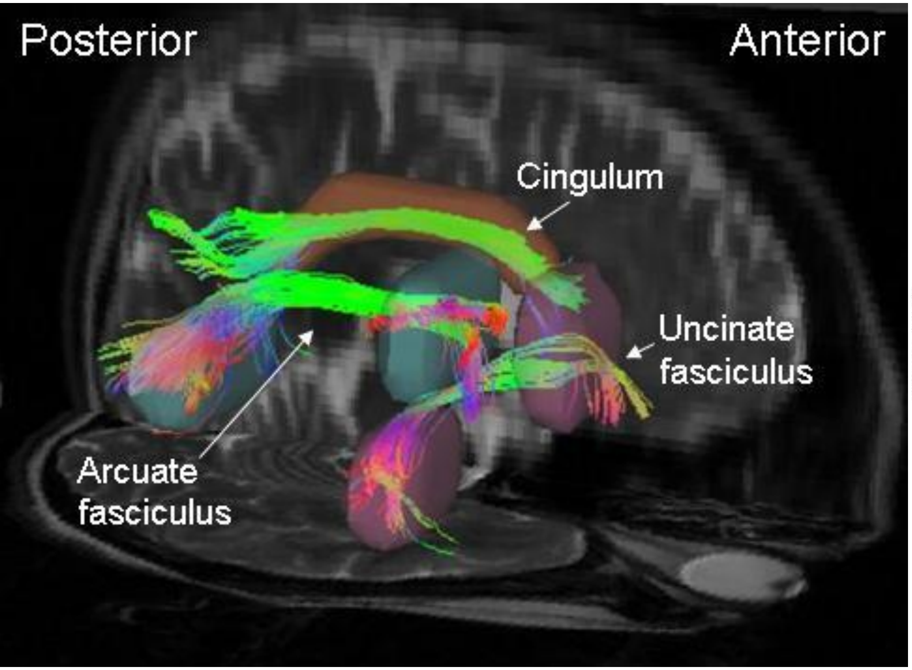

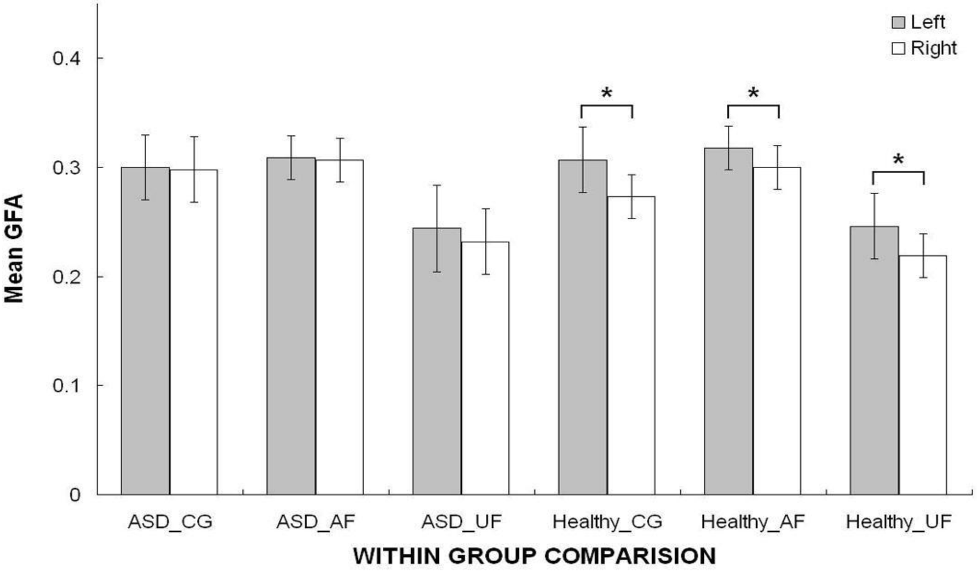

Lo et al. Psych Res Neuroimaging, 2011

Mean Path Algorithm

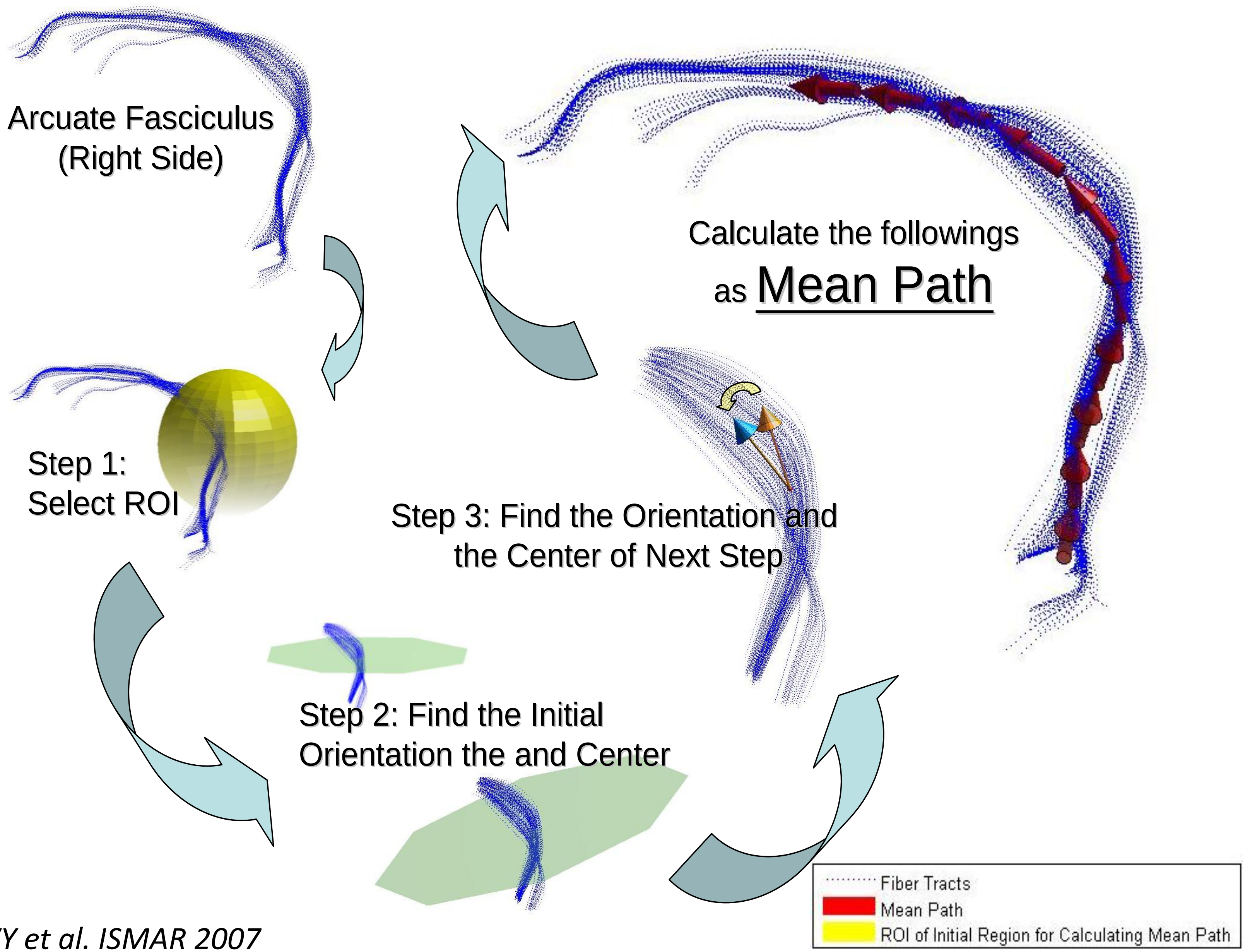

Chiang WY et al. ISMAR 2007

Tract-specific analysis

A

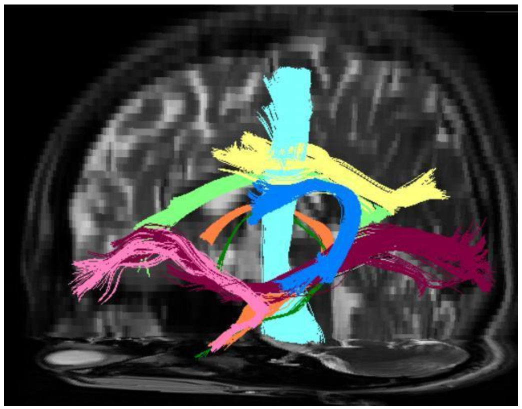

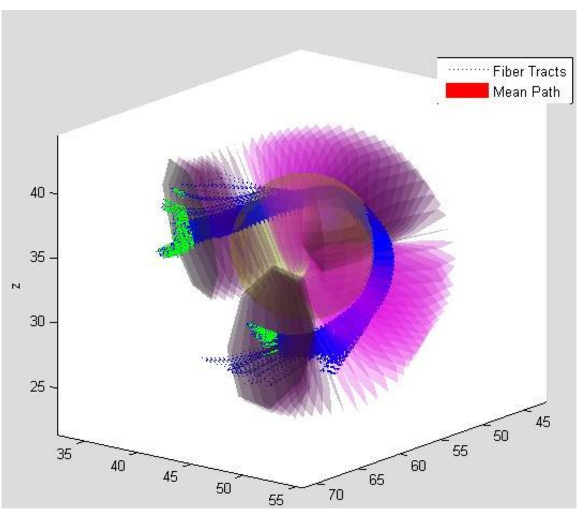

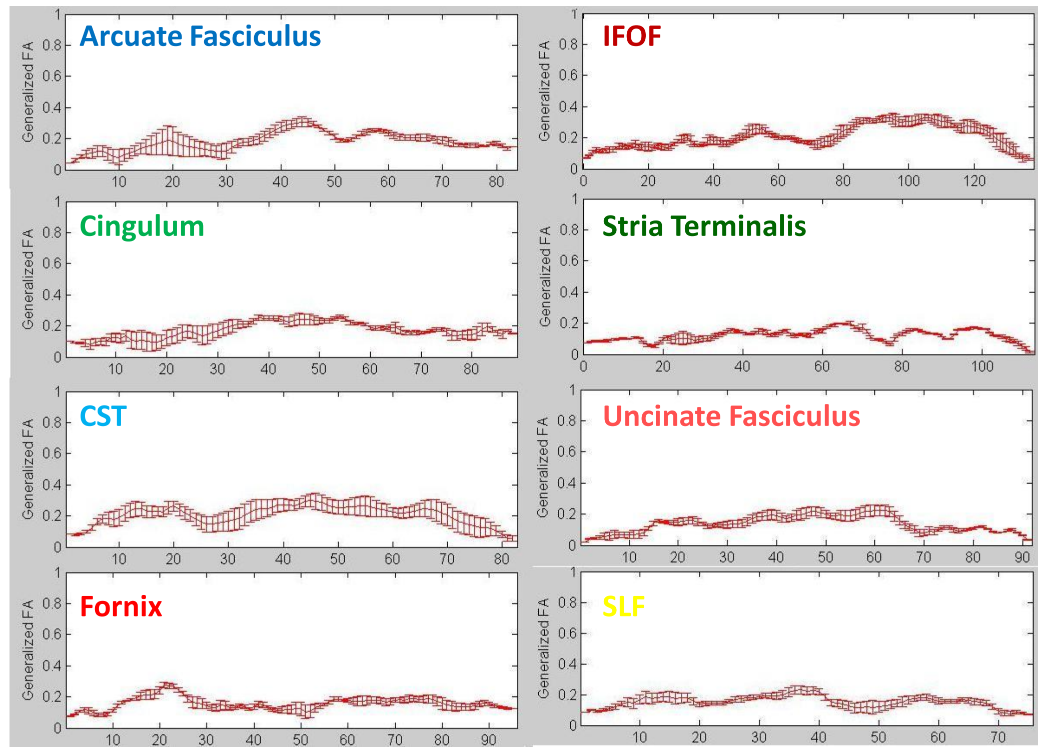

GFA profiles for each fiber tract

Loss of left-greater-than-right asymmetry in autism

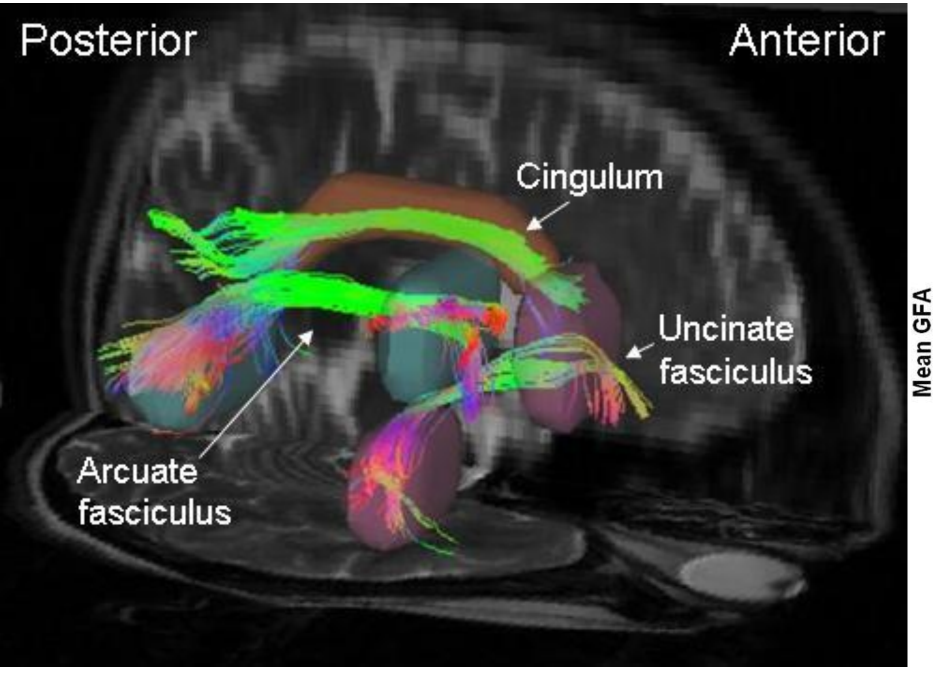

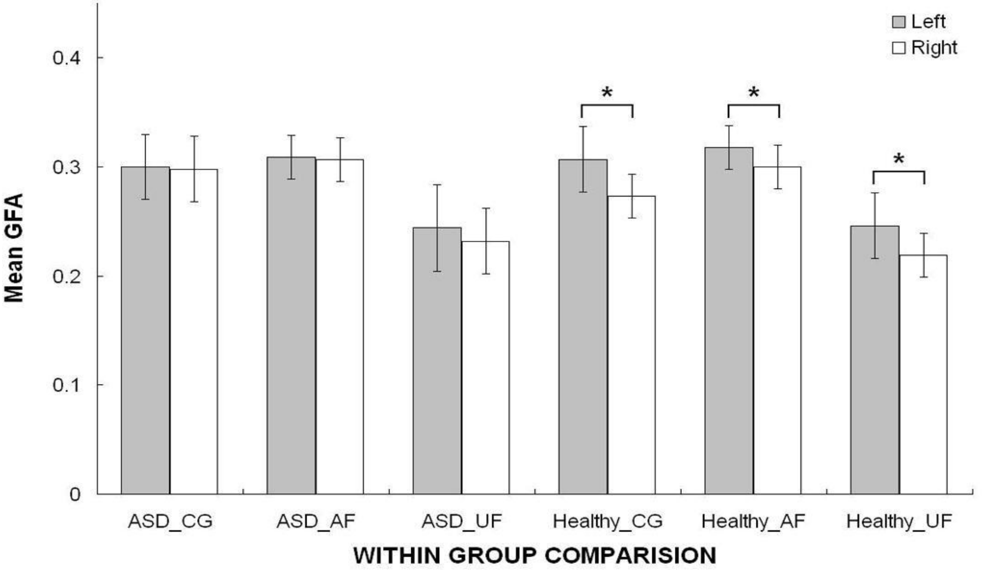

Lo et al. Psych Res Neuroimaging, 2011

DSI template of 122 normal subjects

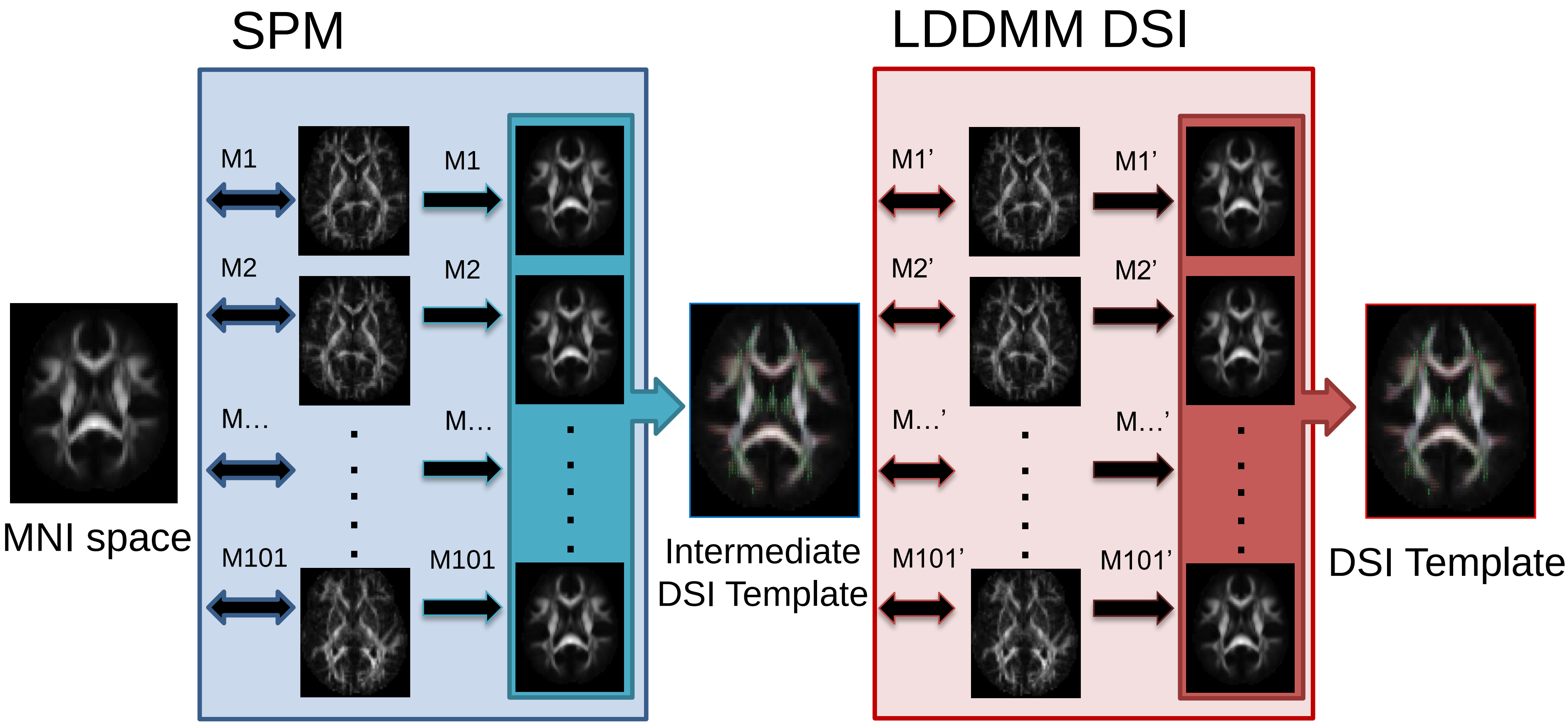

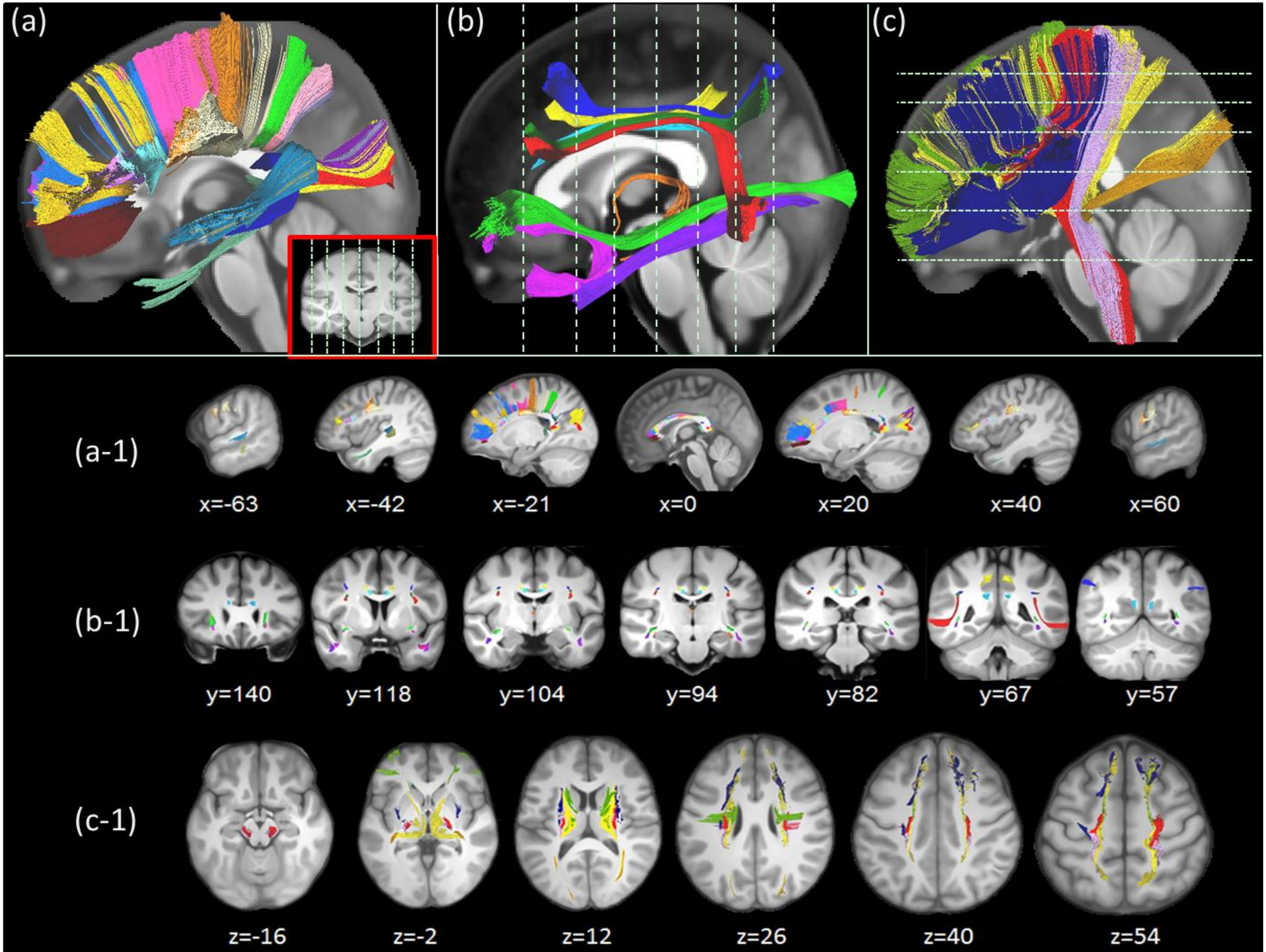
(a)
(b)
(c)
(a-1)
x=-63
x=-42
x=-21
x=0
x=20
x=40
x=60
(b-1)
y=140
y=118
y=104
y=94
y=82
y=67
y=57
(c-1)
z=-16
z=-2
z=12
z=26
z=40
z=54

Association fibers

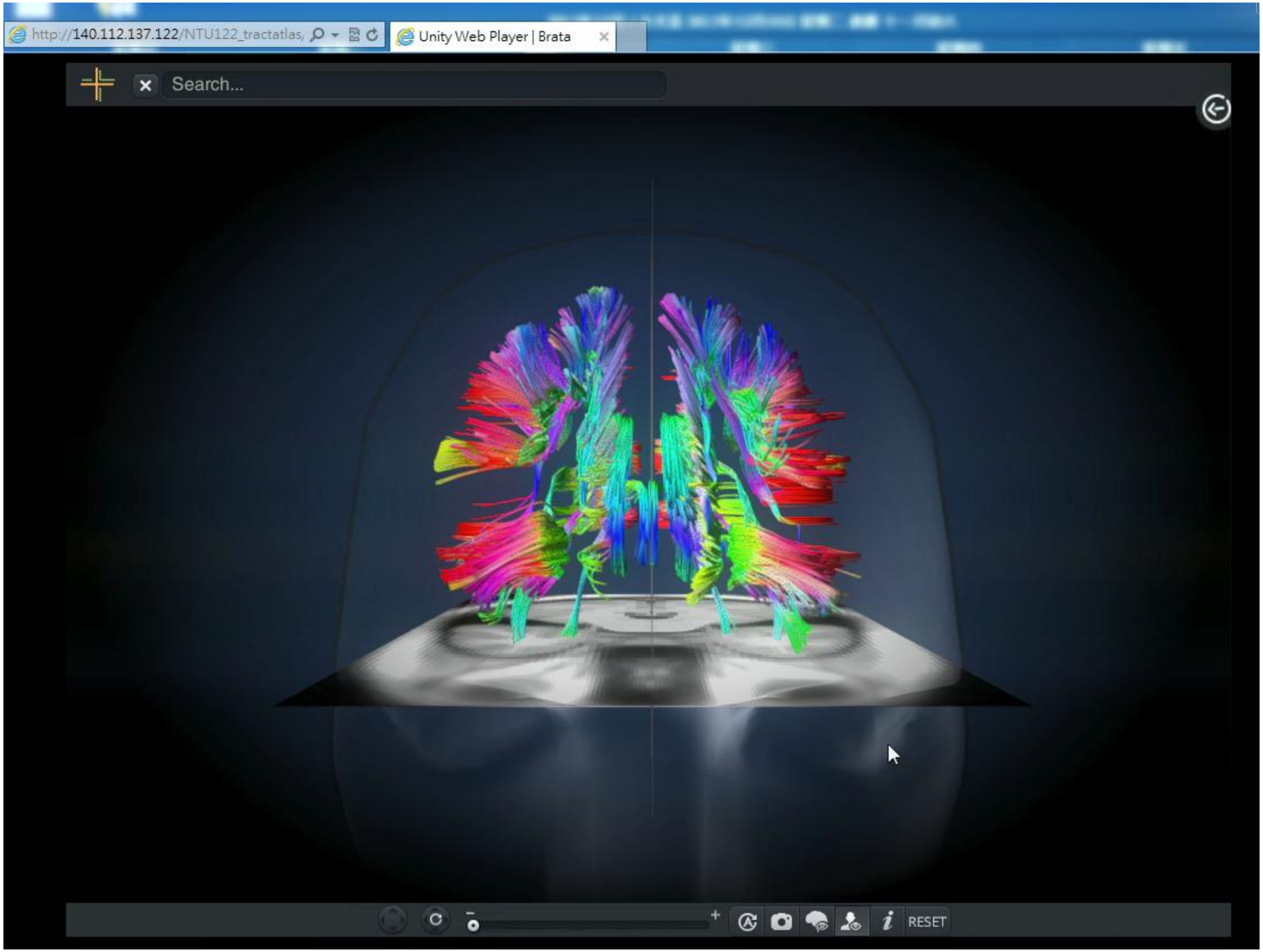

Commissural fibers

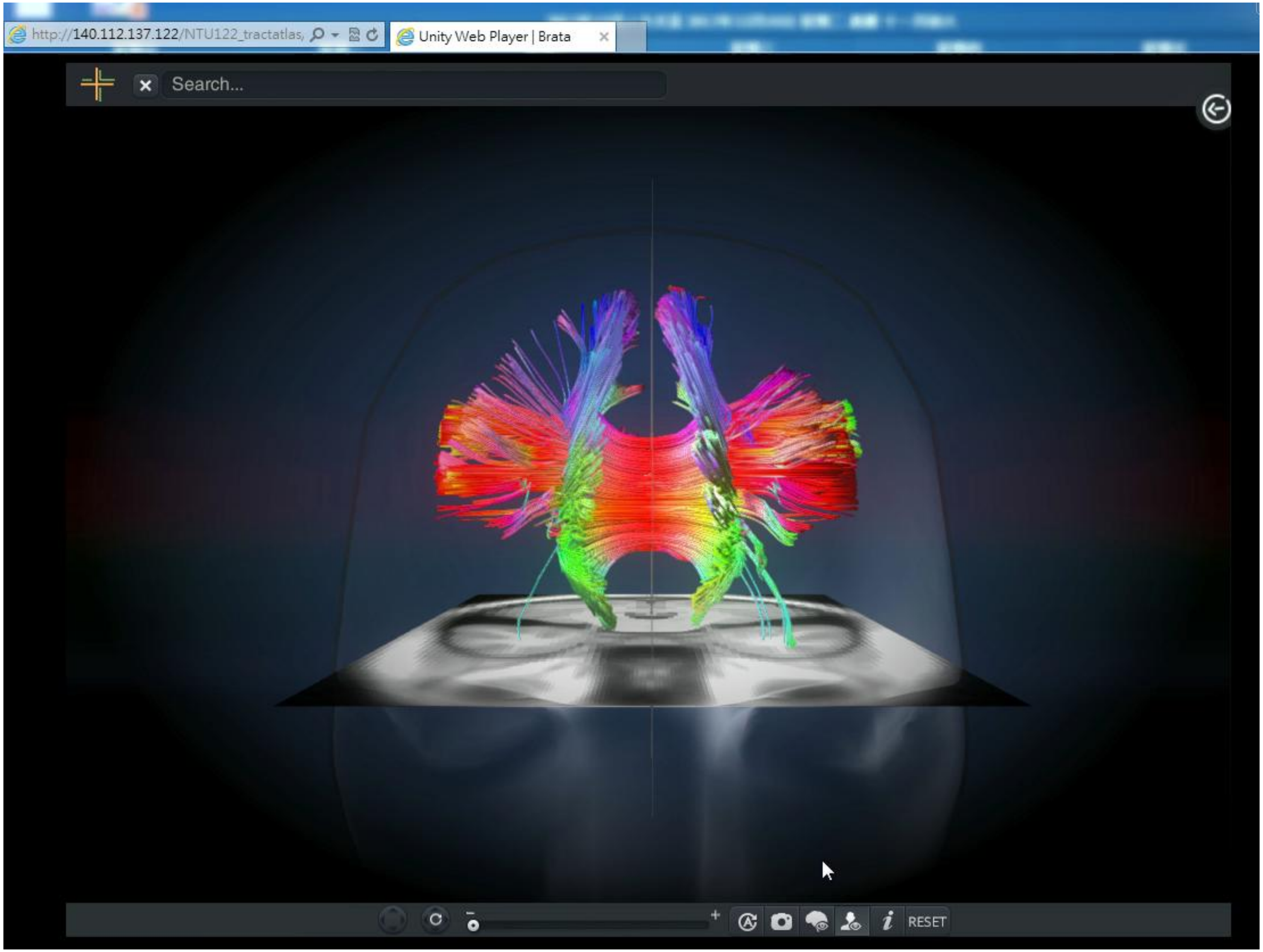

Projection fibers

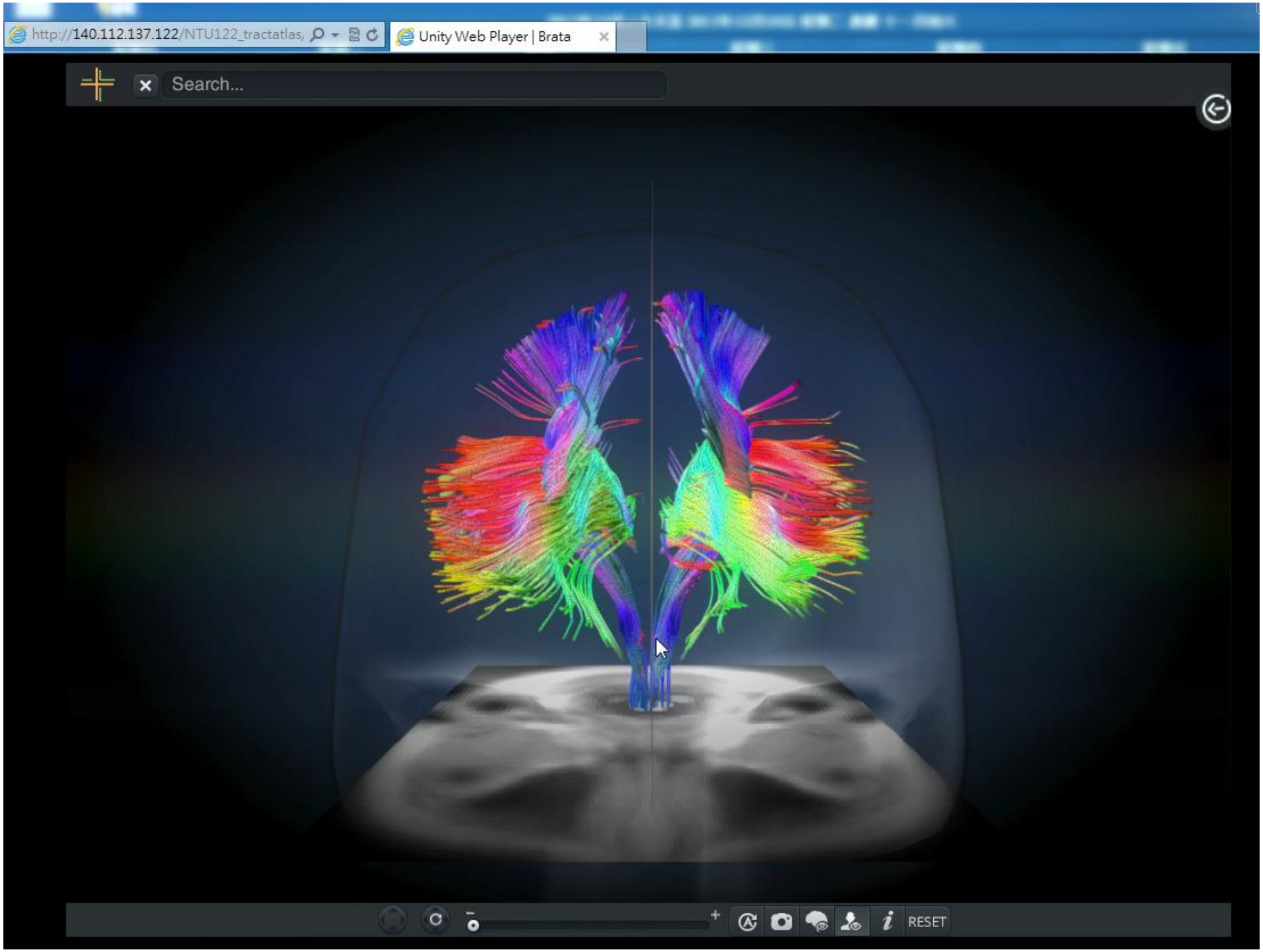

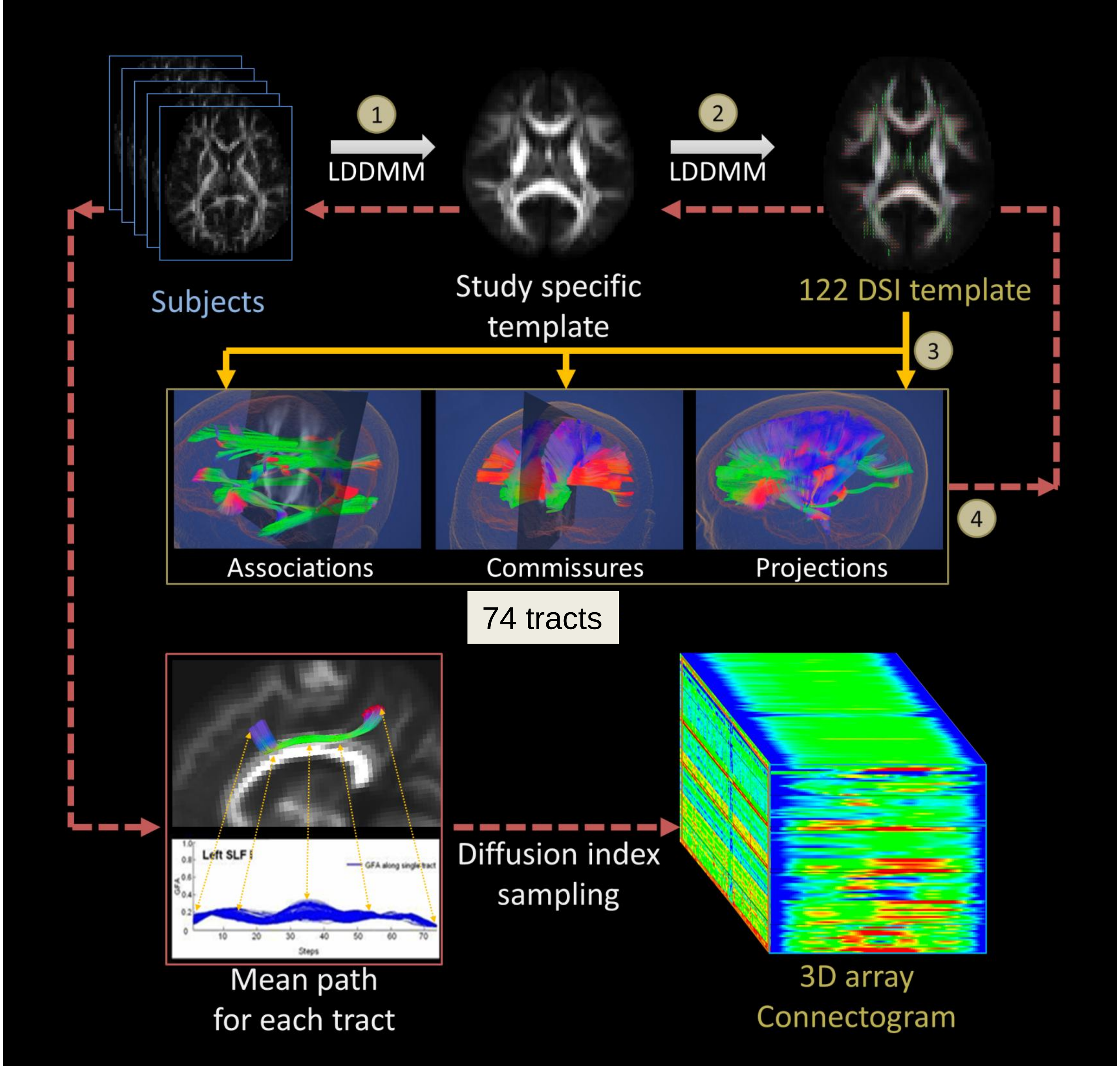

1
LDDMM
2
LDDMM
Subjects
Study specific template
122 DSI template
3
Associations
Commissures
Projections
4
74 tracts
Left SLF I
GFA along single tract
Steps
Diffusion index sampling
Mean path for each tract
3D array Connectogram

An array-based brain connectome

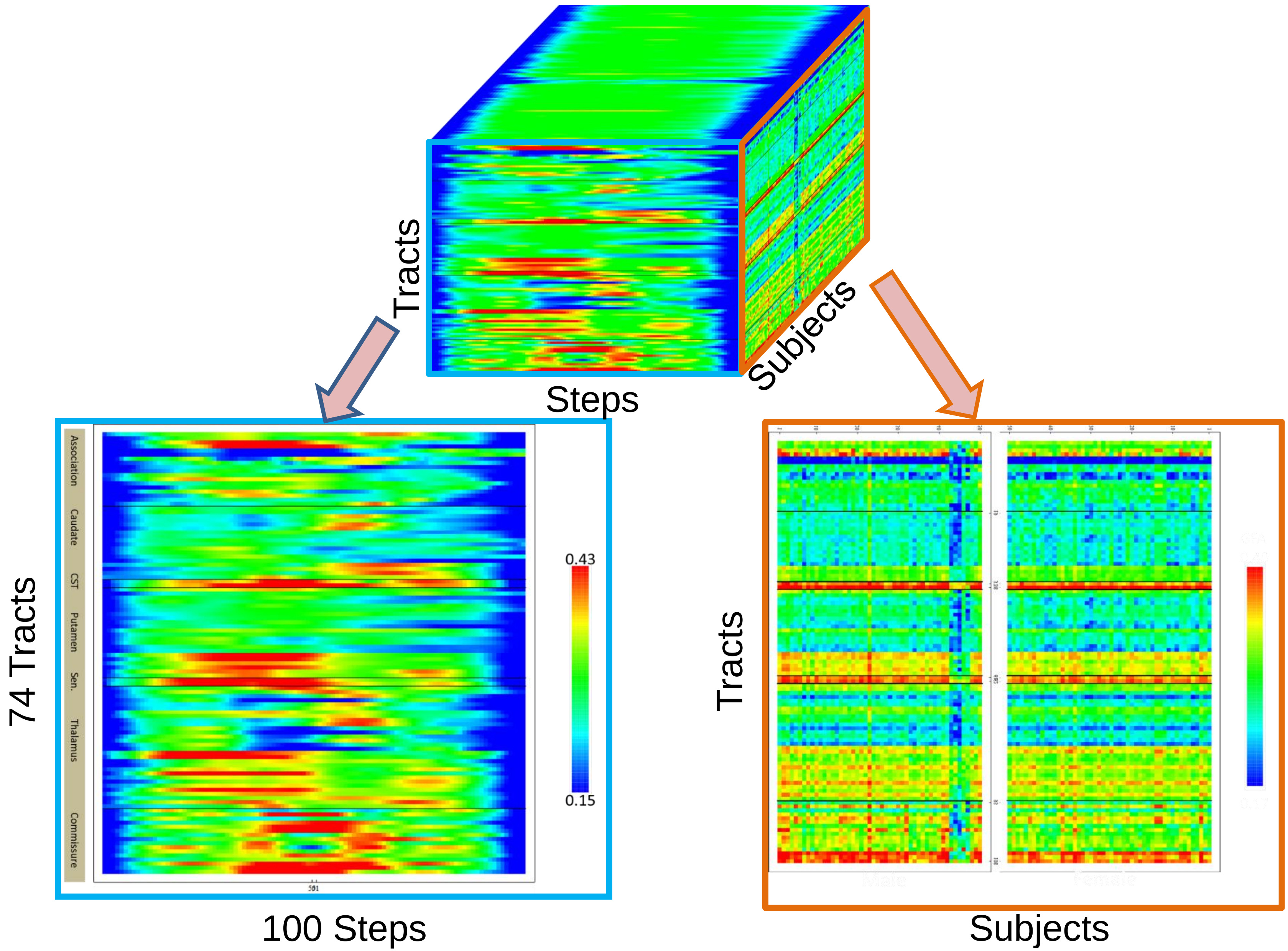

Conclusion

- Diffusion MRI allows us to probe tissue microstructure at microscopic level
  - It is detects cancerous tissue
  - It reveals ingenious design of fiber architecture of the myocardium
  - It allows us to visualize and analysis connectivity of the wired brain
- Therefore, diffusion MRI is a potentially power tool in clinical cancer, cardiac and brain imaging

blog.roodo.com/nashchou/archives/2799081.html